A Sphere Packing Bound for Vector Gaussian Fading Channels Under Peak Amplitude Constraints

Antonino Favano, *Member, IEEE*, Marco Ferrari, *Member, IEEE*, Maurizio Magarini, *Member, IEEE*, and Luca Barletta, *Member, IEEE*

***Abstract*— An upper bound on the capacity of multiple-input multiple-output (MIMO) Gaussian fading channels is derived under peak amplitude constraints. The upper bound is obtained borrowing concepts from convex geometry and it extends to MIMO channels notable results from the geometric analysis on the capacity of scalar Gaussian channels. Relying on a sphere packing argument and on the renowned Steiner's formula, the proposed upper bound depends on the intrinsic volumes of the constraint region, *i.e.*, functionals defining a measure of the geometric features of a convex body. The tightness of the bound is investigated at high signal-to-noise ratio (SNR) for any arbitrary convex amplitude constraint region, for any channel matrix realization, and any dimension of the MIMO system. In addition, two variants of the upper bound are proposed: one is useful to ensure the feasibility in the evaluation of the bound and the other to improve the bound's performance in the low SNR regime. Finally, the upper bound is specialized for two practical transmitter configurations, either employing a single power amplifier for all transmitting antennas or a power amplifier for each antenna.**

***Index Terms*— Fading channels, MIMO systems, peak amplitude constraint, capacity bounds, sphere packing, intrinsic volumes.**

I. Introduction

THE capacity of additive white Gaussian noise (AWGN) channels subject to average power constraints is derived by Shannon in [2] and it is perhaps the most renowned accomplishment in information theory. Its extension to multi-antenna systems is another celebrated result and it is presented in [3] by Telatar. Overall, Gaussian channels under average power constraints have been studied extensively. On the other hand, the capacity of AWGN channels under peak power or peak amplitude constraints is still an ongoing research topic.

In the field of wireless communications, the information capacity of amplitude-constrained channels is of great interest for the following practical reasons. The ever-growing requirements in data rates and the ubiquitous presence of wireless devices have made energy efficiency one of the fundamental features in the design of a wireless communication system. In this regard, one of the main components affecting the efficiency of the whole system is the power amplifier. Its nonlinear characteristic imposes a limit on the peak power of the signals it receives in input. To properly exploit the available resources of a wireless channel, it is fundamental to establish a realistic information theoretic framework, providing an accurate estimate of attainable data rates. By imposing peak power or peak amplitude constraints on the channel input, one can accurately represent the limitations induced by power amplifiers. Wireless communications encompass several practical applications, ranging from microwave wireless to free-space optical communications. For more details on the latter, see [4], [5], [6], [7], [8]. In this work, we will mainly focus on the channel capacity of microwave wireless systems, nevertheless the extension of our results to the free-space optical scenario is straightforward.

The first significant result in the evaluation of the channel capacity under peak amplitude constraints is presented in [9] by Smith. He proves that the capacity-achieving distribution of an amplitude-constrained scalar Gaussian channel is discrete and comprises a finite number of mass points. Similar results on the discreteness of the capacity-achieving distribution are derived in [10], [11], [12], and [13]. In [14], McKellips presents a simple and tight upper bound on the capacity of scalar amplitude-constrained Gaussian channels. The authors of [15] and [16] derive capacity bounds for multiple-input multiple-output (MIMO) systems with identity channel matrix and subject to a peak amplitude constraint that limits the norm of the input vector. In [17] for the same MIMO systems and constraint, we provide further insights into the capacity-achieving input distribution and define an iterative procedure to numerically evaluate an arbitrarily accurate estimate of the channel capacity. As for systems characterized by nonidentity channel matrices, the authors of [18] investigate the capacity of 2×2 MIMO systems for rectangular input constraint regions. Furthermore, in [19]

Manuscript received 17 November 2021; revised 8 June 2022; accepted 20 August 2022. Date of publication 31 August 2022; date of current version 22 December 2022. An earlier version of this paper was presented at the 2020 IEEE Information Theory Workshop [DOI: 10.1109/ITW46852.2021.9457574]. *(Corresponding author: Marco Ferrari.)*

Antonino Favano is with the Dipartimento di Elettronica, Informazione e Bioingegneria, Politecnico di Milano, 20133 Milan, Italy, and also with the Istituto di Elettronica e di Ingegneria dell'Informazione e delle Telecomunicazioni, Consiglio Nazionale delle Ricerche, 20133 Milan, Italy (e-mail: antonino.favano@polimi.it).

Marco Ferrari is with the Istituto di Elettronica e di Ingegneria dell'Informazione e delle Telecomunicazioni, Consiglio Nazionale delle Ricerche, 20133 Milan, Italy (e-mail: marco.ferrari@ieiit.cnr.it).

Maurizio Magarini and Luca Barletta are with the Dipartimento di Elettronica, Informazione e Bioingegneria, Politecnico di Milano, 20133 Milan, Italy (e-mail: maurizio.magarini@polimi.it; luca.barletta@polimi.it).

Communicated by M. Wigger, Associate Editor for Shannon Theory and Information Measures.

Color versions of one or more figures in this article are available at https://doi.org/10.1109/TIT.2022.3203293.

Digital Object Identifier 10.1109/TIT.2022.3203293

the capacity bounds are further generalized for n-dimensional MIMO fading channels subject to any arbitrary peak amplitude constraint. Finally, in [20] we refine the results presented in [19] for two particular constraints of practical interest: One employs a single amplifier for all transmitting antennas, which determines a constraint on the norm of the input vector. We refer to it as *total amplitude* (TA) constraint; the other transmitter configuration employs multiple power amplifiers, one per transmitting antenna. This configuration induces a peak amplitude constraint on each entry of the input vector, which we define as *per-antenna* (PA) constraint. The configuration employing multiple amplifiers is the most common in MIMO systems, while that employing a single power amplifier is crucial when power consumption is a critical feature [21], [22].

Contribution

In this paper, we provide an asymptotically tight upper bound on the capacity of MIMO AWGN fading channels subject to peak amplitude constraints that is based on a sphere packing argument and that greatly improves upon the existing literature. We derive the sphere packing (SP) upper bound by extending the results in [23] to MIMO systems. We prove that the gap between the derived upper bound and the best lower bound from the literature [20], is asymptotically tight. Indeed, as the signal-to-noise ratio (SNR) goes to infinity, the gap between the bounds vanishes for any channel matrix, any dimension of the MIMO system, and any convex constraint region. Moreover, we introduce two variants of the SP upper bound: One is useful to always guarantee a feasible evaluation of the bound while preserving a vanishing capacity gap at high SNR and the other is able to improve the performance at low SNR. We also specialize the SP bound for two practical transmitter configurations.

Structure of the Paper

In Section II, we introduce some useful mathematical tools needed throughout the rest of the paper; in Section III we define the system model; in Section IV we outline previous results present in the current literature; and in Section V we describe the SP upper bound and its variants. In Section VI, we specialize the SP bound for the TA constraint and for the PA constraint. Furthermore, we evaluate the tightness of the resulting capacity bounds and compare it with the main results from previous works. Section VII concludes the paper.

Notation

We use bold letters for vectors ($\mathbf{x}$), uppercase letters for random variables (X), calligraphic uppercase letters for subsets of vector spaces ($\mathcal{X}$), and uppercase sans serif letters for matrices (H). We denote by $\|\mathbf{x}\|$ the Euclidean norm of the vector $\mathbf{x}$, by H^T the transposed of a matrix H, and by $\det(\mathsf{H})$ its determinant. Furthermore, $\mathcal{CN}(\boldsymbol{\mu}, \Sigma)$ indicates a complex multivariate Gaussian distribution with mean vector $\boldsymbol{\mu}$ and covariance matrix Σ. We represent the $n \times 1$ vector of zeros by $\mathbf{0}_n$ and the $n \times n$ identity matrix by I_n. We denote by $\mathcal{B}_n \triangleq \{\mathbf{x} : \|\mathbf{x}\| \leq 1\}$ the n-dimensional unit ball in $\mathbb{R}^n$ centered at $\mathbf{0}_n$ and by $\delta\mathcal{B}_n \triangleq \{\mathbf{x} : \|\mathbf{x}\| \leq \delta\}$ the n-dimensional ball of radius δ centered in $\mathbf{0}_n$. We define the n-dimensional box of sides $\boldsymbol{d}$ as $\mathrm{Box}_n(\boldsymbol{d}) \triangleq \{\mathbf{x} : |x_k| \leq d_k/2,\ k = 1, \ldots, n\}$ and, with a slight abuse of notation, we use $\mathrm{Box}_n(d)$ whenever $d_k = d,\ \forall k$. Finally, we define $\mathsf{H}\mathcal{X} \triangleq \{\mathbf{y} : \mathbf{y} = \mathsf{H}\mathbf{x},\ \mathbf{x} \in \mathcal{X}\}$, we denote the M-times Cartesian product of $\mathsf{H}\mathcal{X}$ with itself by $[\mathsf{H}\mathcal{X}]^{\times \mathsf{M}}$, and the n-dimensional volume of the set $\mathcal{X}$ by $\mathrm{Vol}_n(\mathcal{X})$.

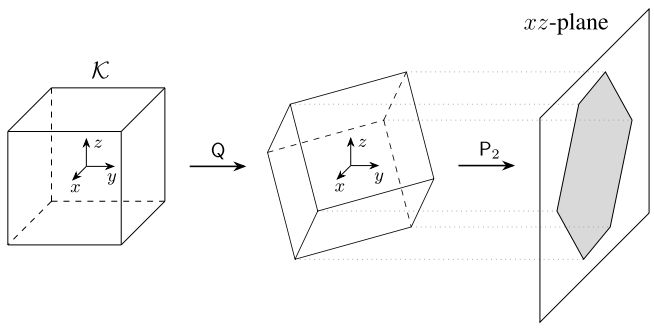

Fig. 1. Example of rotation and projection of a cube $\mathcal{K}$ for the evaluation of the intrinsic volume $\mathrm{V}_2(\mathcal{K})$.

II. Preliminaries

Given two subsets $\mathcal{K}$ and $\mathcal{R}$ of a vector space, the Minkowski sum is denoted by the operator $\oplus$ and it gives the set obtained by adding each vector in $\mathcal{K}$ to each vector in $\mathcal{R}$ as

$$\mathcal{K} \oplus \mathcal{R} \triangleq \{\mathbf{k} + \mathbf{r} \mid \mathbf{k} \in \mathcal{K},\ \mathbf{r} \in \mathcal{R}\}. \tag{1}$$

Moreover, if $\mathcal{K}$ is a convex body in $\mathbb{R}^n$, we denote by $\mathrm{V}_j(\mathcal{K})$ its jth intrinsic volume, with $j = 0, \ldots, n$. Intrinsic volumes are nonnegative, homogeneous, and monotonic functionals and represent a fundamental measure of content for a convex body [24]. The authors of [24] also provide an intuitive, yet technical, definition as follows. Let P_j be an $n \times n$ orthogonal projection matrix, projecting onto a fixed j-dimensional subspace of $\mathbb{R}^n$. Furthermore, let Q be an $n \times n$ random rotation matrix drawn uniformly from the Haar measure[1] on the compact, homogeneous group of $n \times n$ orthogonal matrices with determinant one. Then, the intrinsic volumes of a convex body $\mathcal{K}$ are defined as

$$\mathrm{V}_j(\mathcal{K}) \triangleq \binom{n}{j} \frac{\kappa_n}{\kappa_j \kappa_{n-j}} \mathsf{E}\left[\mathrm{Vol}_j(\mathsf{P}_j \mathsf{Q} \mathcal{K})\right], \quad j = 0, \ldots, n, \tag{2}$$

where the expectation is taken with respect to the random rotation matrix Q and where $\kappa_i \triangleq \pi^{\frac{i}{2}}/\Gamma\left(\frac{i}{2} + 1\right)$ is the volume of the i-dimensional unit ball. We remark that from (2), it is straightforward to see that the nth intrinsic volume of $\mathcal{K}$ coincides with its volume $\mathrm{Vol}_n(\mathcal{K})$. Some other special cases are $2\mathrm{V}_{n-1}(\mathcal{K})$ being the surface area of $\mathcal{K}$, $2\mathrm{V}_1(\mathcal{K})\,\kappa_{n-1}/(n\kappa_n)$ being the mean width, and $\mathrm{V}_0(\mathcal{K}) = 1$ being the Euler characteristic [26]. Aside from a scaling factor, the jth intrinsic volume $\mathrm{V}_j(\mathcal{K})$ is obtained by evaluating an expected value on j-dimensional volumes. For example, consider $\mathcal{K}$ being a cube. In Fig. 1, we show the effect of one random realization of Q,

[1]For a rigorous definition of the Haar measure, see [25].

as in (2) for $\mathrm{V}_2(\mathcal{K})$. The matrix Q applies a random rotation to the cube and the matrix P_2 projects it onto a plane. Therefore, the volume $\mathrm{Vol}_2(\mathsf{P}_2\mathsf{Q}\mathcal{K})$ is the measure of the gray area in Fig. 1. For further detail on intrinsic volumes see [24], [26], [27], [28]. Intrinsic volumes are characterized by the following property

$$\mathrm{V}_j(\mathsf{A}\mathcal{K}) = \mathsf{A}^j \mathrm{V}_j(\mathcal{K}),\ \mathsf{A} \geq 0,\ \forall j. \tag{3}$$

Given a set $\mathcal{K}$ such that $\mathcal{K} \supset \mathcal{R}$, it holds

$$\mathrm{V}_j(\mathcal{K}) \geq \mathrm{V}_j(\mathcal{R}),\ \forall j. \tag{4}$$

Thanks to Steiner's formula [23, Theorem 4] we can evaluate the n-dimensional volume of the Minkowski sum between a convex set $\mathcal{K}$ and a ball of radius $\delta \geq 0$ as follows

$$\mathrm{Vol}_n(\mathcal{K} \oplus \delta\mathcal{B}_n) = \sum_{j=0}^{n} \mathrm{V}_j(\mathcal{K})\, \mathrm{Vol}_{n-j}(\delta\mathcal{B}_{n-j}). \tag{5}$$

Since the right-hand side of (5) is a convolution, it is useful to introduce the (logarithmic) generating function of the intrinsic volumes of $\mathcal{K}$ as [23, Theorem 8]

$$G_{\mathcal{K}}(t) = \log\left(\sum_{j=0}^{n} \mathrm{V}_j(\mathcal{K})\, e^{jt}\right). \tag{6}$$

As shown in [24], an important property of these generating functions is that, given two sets $\mathcal{K}$ and $\mathcal{R}$, it holds

$$G_{\mathcal{K}\times\mathcal{R}}(t) = G_{\mathcal{K}}(t) + G_{\mathcal{R}}(t),\ \forall t \in \mathbb{R}. \tag{7}$$

Let us denote by $\mathcal{T}$ a topological vector space and by $\mathcal{T}^*$ the corresponding dual vector space, i.e., the set of all linear forms on $\mathcal{T}$. Given a function $f : \mathcal{T} \to \mathbb{R} \cup \{-\infty, +\infty\}$, by following [29] we define the convex conjugate of f as $f^* : \mathcal{T}^* \to \mathbb{R} \cup \{-\infty, +\infty\}$ such that

$$f^*(t^*) \triangleq \sup_{t\in\mathcal{T}} \{t \cdot t^* - f(t)\}. \tag{8}$$

III. Channel Model

Let us consider an $\mathsf{N} \times \mathsf{N}$ complex MIMO channel with input-output relationship given by

$$\widetilde{\mathbf{Y}} = \widetilde{\mathsf{H}} \cdot \widetilde{\mathbf{X}} + \widetilde{\mathbf{Z}}. \tag{9}$$

The input vector $\widetilde{\mathbf{X}}$ is such that $\widetilde{\mathbf{X}} \in \widetilde{\mathcal{X}}$, with $\widetilde{\mathcal{X}}$ being a convex constraint region, $\widetilde{\mathbf{Z}} \sim \mathcal{CN}(\mathbf{0}_{\mathsf{N}}, 2\sigma_z^2 \mathsf{I}_{\mathsf{N}})$ is the additive noise vector, and $\widetilde{\mathsf{H}}$ is any full rank channel fading matrix. We assume $\widetilde{\mathsf{H}}$ to be constant throughout the channel uses and known both at the transmitter and at the receiver. Let us vectorize the system in (9) in its real and imaginary components. We obtain the equivalent model

$$\mathbf{Y} = \mathsf{H} \cdot \mathbf{X} + \mathbf{Z}, \tag{10}$$

with $\mathsf{H} = \mathrm{Re}\{\widetilde{\mathsf{H}}\} \otimes \mathsf{I}_2 + \mathrm{Im}\{\widetilde{\mathsf{H}}\} \otimes \left[\begin{smallmatrix} 0 & -1 \\ 1 & 0 \end{smallmatrix}\right]$, where the operator $\otimes$ is the Kronecker product, $\mathbf{Y}$ is a $2\mathsf{N} \times 1$ vector defined as $\mathbf{Y} = [\mathrm{Re}\{\widetilde{Y}_1\}, \mathrm{Im}\{\widetilde{Y}_1\}, \ldots, \mathrm{Re}\{\widetilde{Y}_{\mathsf{N}}\}, \mathrm{Im}\{\widetilde{Y}_{\mathsf{N}}\}]^T$, and analogously for $\mathbf{X}$ and $\mathbf{Z}$.

We define the MIMO channel capacity as

$$\mathsf{C}\left(\mathcal{X}, \mathsf{H}, \sigma_z^2\right) \triangleq \sup_{F_{\mathbf{X}}:\, \mathrm{supp}(F_{\mathbf{X}}) \subseteq \mathcal{X}} \mathrm{I}(\mathbf{X}; \mathbf{Y}) \tag{11}$$

$$= \sup_{F_{\mathbf{X}}:\, \mathrm{supp}(F_{\mathbf{X}}) \subseteq \mathcal{X}} \{\mathrm{h}(\mathbf{Y})\} - \mathrm{h}(\mathbf{Z}), \tag{12}$$

where $F_{\mathbf{X}}$ is the input distribution law and $\mathcal{X}$ is the equivalent input constraint region derived from $\widetilde{\mathcal{X}}$. Notice that we consider a system with a number of transmitting antennas, N_T, equal to the number of receiving antennas, N_R. Nonetheless, the authors of [5] show that any channel such that $\mathrm{rank}(\widetilde{\mathsf{H}}) \leq \mathsf{N}_T \leq \mathsf{N}_R$ can be transformed into an equivalent $\mathrm{rank}(\widetilde{\mathsf{H}}) \times \mathsf{N}_T$ MIMO channel. Therefore, when $\mathrm{rank}(\widetilde{\mathsf{H}}) = \mathsf{N}_T$ we can still equivalently use the model in (9). On the other hand, when $\mathrm{rank}(\widetilde{\mathsf{H}}) < \mathsf{N}_T$, the model in (9) is not valid anymore and therefore our results cannot be trivially extended to this case (see [5] for further detail). Since we investigate the capacity of amplitude-constrained channels, it is convenient to define the SNR as the ratio between the peak power of the input vector and the trace of the noise covariance matrix. Then, the SNR depends on the specific constraint region $\mathcal{X}$ as $\mathrm{SNR} \triangleq (r_{\max}(\mathcal{X}))^2/(2\mathsf{N}\sigma_z^2)$, with $r_{\max}(\mathcal{X}) \triangleq \sup_{\mathbf{x}\in\mathcal{X}} \{\|\mathbf{x}\|\}$.

IV. Previously Proposed Bounds

In [19], the authors provide capacity upper and lower bounds for AWGN MIMO systems under an arbitrary peak amplitude constraint region $\mathcal{X}$ and for any channel matrix, known at both the transmitter and the receiver. Their duality upper bounds are derived by considering an enlarged output constraint region $\mathcal{D} \supset \mathsf{H}\mathcal{X}$. Although there are some specific constraints $\mathcal{X}$ for which one can still use a duality approach directly tailored on $\mathsf{H}\mathcal{X}$, e.g. as in [5], this is not always the case. Whenever tailored approaches are not viable, a suboptimal but effective solution is to consider an enlarged constraint region $\mathcal{D}$ designed to make the derivation of an upper bound feasible. Specifically, in [19] they consider $\mathcal{D}$ to be either a ball or a box. Let $\mathcal{D}_1$ be the $(2\mathsf{N})$-dimensional ball of radius $d_1 = r_{\max}(\mathsf{H}\mathcal{X})$ and $\mathcal{D}_2 = \mathrm{Box}_{2\mathsf{N}}(\mathbf{d}_2)$ be the smallest box containing $\mathsf{H}\mathcal{X}$. Then, in [19, Theorem 10] the authors define their duality upper bounds as follows

$$\mathsf{C} \leq \overline{\mathsf{C}}_{\mathrm{D},1} \triangleq \log\left(c_{2\mathsf{N}}(d_1) + \frac{\mathrm{Vol}_{2\mathsf{N}}(\mathcal{D}_1)}{(2\pi e\sigma_z^2)^{\mathsf{N}}}\right), \tag{13}$$

where $c_{2\mathsf{N}}(d_1) = \sum_{j=0}^{2\mathsf{N}-1} \binom{2\mathsf{N}-1}{j} \frac{\Gamma(\mathsf{N}-j/2)}{2^{j/2}\Gamma(\mathsf{N})} (d_1/\sigma_z)^j$ and

$$\mathsf{C} \leq \overline{\mathsf{C}}_{\mathrm{D},2} \triangleq \sum_{j=1}^{2\mathsf{N}} \log\left(1 + \frac{d_{2,j}}{\sqrt{2\pi e\sigma_z^2}}\right), \tag{14}$$

where $d_{2,j}$ is the jth component of $\mathbf{d}_2$. The main disadvantage of these bounds is that the more $\mathcal{D}$ differs from $\mathsf{H}\mathcal{X}$, the less accurate the bounds become. In [20], by extending the McKellips-Type upper bound of [16] to MIMO systems affected by fading, we improve the results of [19] for specific cases of the PA constraint and for the TA constraints. Loosely speaking, we achieve better results than those in [19] by considering an upper bound that depends on a smaller constraint region $\mathcal{S}$ such that $\mathcal{D} \supset \mathcal{S} \supset \mathsf{H}\mathcal{X}$. Although, at high SNR, the

resulting asymptotic capacity gap in [20] is smaller compared to the past literature, it can be far from zero. Moreover, the capacity gap widens as N grows larger and the derived upper bounds are valid just for the mentioned specific cases.

In the next section, we propose an upper bound that improves upon those of [20] and that is also far more general. Indeed, as for the duality upper bounds in [19], the proposed bound can be applied to any convex constraint region. Furthermore, we prove that our upper bound provides an asymptotic gap equal to zero for any convex constraint region, any channel matrix H, and any MIMO dimension N.

V. Sphere Packing Upper Bound

In [23], the authors investigate the capacity of AWGN scalar channels under average and peak power constraints. They provide an upper bound based on an SP argument by using a fundamental result from convex geometry, *i.e.*, the Steiner's formula in (5). Given $n \to \infty$ channel uses and the corresponding n-dimensional constraint region $\mathcal{K}$, the authors of [23] define an upper bound that, roughly speaking, is given by $\limsup_{n\to\infty} \frac{1}{n} \log\left(\mathrm{Vol}_n\left(\mathcal{K} \oplus \delta\mathcal{B}_n\right)/\mathrm{Vol}_n\left(\delta\mathcal{B}_n\right)\right)$, where $\delta = \sqrt{n\sigma_z^2}$ and $\delta\mathcal{B}_n$ is the noise ball. Intuitively, the Minkowski sum $\mathcal{K} \oplus \delta\mathcal{B}_n$ is obtained by taking the union of an infinite number of noise balls $\delta\mathcal{B}_n$, after centering them at each point of $\mathcal{K}$. In this work, we extend their upper bound to MIMO fading channels subject to peak amplitude constraints. To do so, let us consider $n = 2\mathsf{N}\cdot\mathsf{M}$. Then, we can reinterpret the n channel uses as M uses of a $(2\mathsf{N})$-dimensional MIMO channel. Since MIMO channel uses are independent, the overall constraint region $\mathcal{K}$ is given by the M-fold Cartesian product of the output signal space, i.e., $\mathcal{K} = [\mathsf{H}\mathcal{X}]^{\times\mathsf{M}}$.

Theorem 1: By considering an arbitrarily large number, M, of independent channel uses, for $\mathsf{M} \to \infty$, the SP bound is

$$\mathsf{C} \le \overline{\mathsf{C}}_{\text{SP}} \triangleq \ell(\sigma_z^2) - \mathsf{N}\log\left(2\pi e\sigma_z^2\right), \tag{15}$$

where $\ell(\sigma_z^2)$ is

$$\ell(\sigma_z^2) = \sup_{\theta\in[0,1]} \left\{ -\sup_t \left\{ 2\mathsf{N}\theta t - \log\left(\sum_{j=0}^{2\mathsf{N}} \mathrm{V}_j\left(\mathsf{H}\mathcal{X}\right) e^{jt}\right)\right\} + (1-\theta)\mathsf{N}\log\frac{2\pi e\sigma_z^2}{1-\theta}\right\}. \tag{16}$$

Proof: See Appendix A. □

Remark 1: Since $\mathsf{h}\left(\mathbf{Z}\right) = \mathsf{N}\log\left(2\pi e\sigma_z^2\right)$, by (15) and (12) it holds that

$$\sup_{F_{\mathbf{X}}:\, \mathrm{supp}(F_{\mathbf{X}})\subseteq\mathcal{X}} \mathsf{h}\left(\mathbf{Y}\right) \le \ell(\sigma_z^2). \tag{17}$$

Let us now evaluate the asymptotic gap between the SP bound $\overline{\mathsf{C}}_{\text{SP}}$ and the entropy power inequality (EPI) lower bound, which is derived in [19] as

$$\underline{\mathsf{C}}_{\text{EPI}} = \mathsf{N}\log\left(1 + \frac{\left(\mathrm{Vol}_{2\mathsf{N}}\left(\mathsf{H}\mathcal{X}\right)\right)^{\frac{1}{\mathsf{N}}}}{2\pi e\sigma_z^2}\right). \tag{18}$$

Proposition 1: The asymptotic capacity gap between the SP upper bound and the EPI lower bound at high SNR is zero

$$g_{\text{SP}} \triangleq \lim_{\sigma_z^2\to 0} \overline{\mathsf{C}}_{\text{SP}} - \underline{\mathsf{C}}_{\text{EPI}} = 0. \tag{19}$$

Proof: See Appendix B. □

Therefore, we have proved that the SP upper bound is asymptotically tight at high SNR for any dimension N of the MIMO system, any channel matrix H, and any convex constraint region $\mathcal{X}$.

A. Generalized Sphere Packing

A practical issue in the evaluation of the SP upper bound is that it is not always trivial to derive the intrinsic volumes of a given region. Furthermore, even when the intrinsic volumes of $\mathcal{X}$ are known, the distortion induced by the channel matrix H can anyway make the evaluation of the intrinsic volumes of $\mathsf{H}\mathcal{X}$ quite complicated, if not unfeasible. Therefore, in this subsection we introduce a further upper bound on the SP approach, which can always be evaluated as long as the $(2\mathsf{N})$th intrinsic volume of $\mathsf{H}\mathcal{X}$, i.e., $\mathrm{Vol}\left(\mathsf{H}\mathcal{X}\right)$, is known.

The core idea is somewhat reminiscent of the one used in the upper bounds of [19]. To evaluate their duality upper bounds, the authors of [19] replace $\mathsf{H}\mathcal{X}$ with a region $\mathcal{D} \supset \mathsf{H}\mathcal{X}$. Roughly speaking, introducing the region $\mathcal{D}$ is similar to replacing all the intrinsic volumes of $\mathsf{H}\mathcal{X}$ with $\mathrm{V}_j\left(\mathcal{D}\right) \ge \mathrm{V}_j\left(\mathsf{H}\mathcal{X}\right)$. Instead, in our generalized sphere packing (G-SP) approach, we are free to upper-bound each $\mathrm{V}_j\left(\mathsf{H}\mathcal{X}\right)$ independently. Aside from the derived improved flexibility, the G-SP approach is especially useful because it allows us to keep the $(2\mathsf{N})$th intrinsic volume of $\mathsf{H}\mathcal{X}$ unaltered, which lets us retain the desirable asymptotic properties of the SP upper bound. We remark that $\mathrm{V}_0\left(\mathcal{K}\right) = 1$ for any $\mathcal{K}$ and that $\mathrm{V}_{2\mathsf{N}}\left(\mathsf{H}\mathcal{X}\right) = \det\left(\mathsf{H}\right)\mathrm{Vol}_{2\mathsf{N}}\left(\mathcal{X}\right)$ can be typically evaluated. Instead, for the $\mathrm{V}_j\left(\mathsf{H}\mathcal{X}\right)$'s, with $j = 1,\ldots,2\mathsf{N}-1$, we can always define an upper bound by choosing, for each j, an appropriate region $\mathcal{S}_j \supset \mathsf{H}\mathcal{X}$, which by (4) guarantees that $\mathrm{V}_j\left(\mathcal{S}_j\right) \ge \mathrm{V}_j\left(\mathsf{H}\mathcal{X}\right)$. Therefore, we have

$$\mathrm{V}_j\left(\mathsf{H}\mathcal{X}\right) \le \overline{\mathrm{V}}_j \triangleq \begin{cases} 1, & j = 0 \\ \mathrm{V}_j\left(\mathcal{S}_j\right), & j = 1,\ldots,2\mathsf{N}-1 \\ \det\left(\mathsf{H}\right)\mathrm{Vol}_{2\mathsf{N}}\left(\mathcal{X}\right), & j = 2\mathsf{N}. \end{cases} \tag{20}$$

Note that the choice of $\mathcal{S}_j$ depends on the considered $\mathsf{H}\mathcal{X}$. Some practical choices of $\mathcal{S}_j$ for which intrinsic volumes can be either derived or numerically evaluated are balls, boxes, ellipsoids, or Cartesian products of these.

Lemma 1: By considering the upper bounds $\overline{\mathrm{V}}_j$ on the intrinsic volumes of $\mathsf{H}\mathcal{X}$ and an arbitrarily large number, M, of independent channel uses, for $\mathsf{M} \to \infty$, the G-SP upper bound is

$$\mathsf{C} \le \overline{\mathsf{C}}_{\text{G-SP}} \triangleq \ell_{\text{G}}(\sigma_z^2) - \mathsf{N}\log\left(2\pi e\sigma_z^2\right), \tag{21}$$

where $\ell_{\text{G}}(\sigma_z^2)$ is

$$\ell_{\text{G}}(\sigma_z^2) \triangleq \sup_{\theta\in[0,1]} \left\{ -\sup_t \left\{ 2\mathsf{N}\theta t - \log\left(\sum_{j=0}^{2\mathsf{N}} \overline{\mathrm{V}}_j e^{jt}\right)\right\} + (1-\theta)\mathsf{N}\log\frac{2\pi e\sigma_z^2}{1-\theta}\right\}. \tag{22}$$

Proof: The proof is almost identical to that of Theorem 1. The only difference is that instead of the true intrinsic volumes,

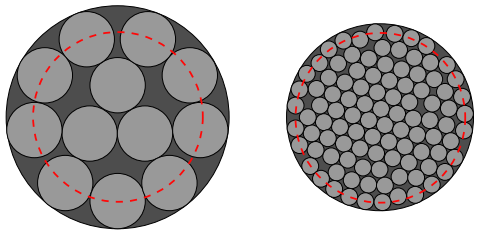

Fig. 2. Two sphere packing examples under a peak amplitude constraint and different SNR values. For both cases, the red dashed line is the border of $\mathcal{K} = \mathcal{B}_2$, in dark gray the result of the Minkowski sum between $\mathcal{K}$ and the noise ball for each specific SNR. On the left, the light gray noise balls are translated replicas of $\delta_1 \mathcal{B}_2$, while on the right of $\delta_2 \mathcal{B}_2$ with $\delta_1 > \delta_2$.

we consider the upper bounds $\overline{\mathrm{V}}_j$'s defined in (20). Notice that, since the logarithm is a monotonic function and the intrinsic volumes in (74) are nonnegative coefficients in a sum of exponentials, it holds $\ell_{\mathrm{G}}(\sigma_z^2) \geq \ell(\sigma_z^2)$ and therefore $\mathsf{C} \leq \overline{\mathsf{C}}_{\text{SP}} \leq \overline{\mathsf{C}}_{\text{G-SP}}$. □

Proposition 2: The asymptotic capacity gap between the G-SP upper bound and the EPI lower bound at high SNR is zero

$$g_{\text{G-SP}} \triangleq \lim_{\sigma_z^2 \to 0} \overline{\mathsf{C}}_{\text{G-SP}} - \underline{\mathsf{C}}_{\text{EPI}} = 0. \tag{23}$$

Proof: As σ_z^2 goes to zero we get the same result of (82) for $\ell_{\mathrm{G}}(\sigma_z^2)$ as well. Then, the G-SP upper bound asymptotically depends uniquely on the $(2\mathsf{N})$th intrinsic volume, which by (20) is still $\mathrm{V}_{2\mathsf{N}}(\mathsf{H}\mathcal{X})$ and therefore determines the same vanishing gap of (19). □

B. Piecewise Sphere Packing

Although the SP and G-SP upper bounds are asymptotically tight, they can be loose at low SNR. Indeed, since the SP bound is based on geometric arguments, its accuracy depends on how precisely the Minkowski sum approximates the true channel output region. As already mentioned, the Minkowski sum in (46) is obtained by taking the union of an infinite number of noise balls, centered at each point of $[\mathsf{H}\mathcal{X}]^{\times \mathsf{M}}$. On the other hand, a rigorous application of the sphere packing problem considers the union of nonoverlapping replicas of $\delta\mathcal{B}_n$, packed in $[\mathsf{H}\mathcal{X}]^{\times \mathsf{M}} \oplus \delta\mathcal{B}_n$. Roughly speaking, the Minkowski sum provides an upper bound by allowing the noise balls to overlap. Therefore, it is intuitive that, as the noise balls get smaller, the Minkowski sum becomes a better approximation of the output signal space $[\mathsf{H}\mathcal{X}]^{\times \mathsf{M}}$, as shown in Fig. 2. At the same time, Fig. 2 also shows that the Minkowski sum can be far from an ideal approximation at low SNR. We now derive a family of piecewise sphere packing (P-SP) upper bounds that is able to improve upon the standard SP bound in (15) in the mentioned SNR range.

Lemma 2: Let us consider $r \triangleq r_{\max}(\mathcal{X})$ and the singular value decomposition of $\mathsf{H} = \mathsf{U}\Lambda\mathsf{V}^T$. Let us denote the diagonal elements of Λ by $\lambda_1, \ldots, \lambda_{2\mathsf{N}}$ and assume that $\lambda_1 \geq \lambda_2 \geq \cdots \geq \lambda_{2\mathsf{N}}$, since it is always possible to rearrange the MIMO system in such a way that this condition is satisfied. Given any combination of positive integers u and l with sum equal to $2\mathsf{N}$ and by considering an arbitrarily large number, M, of independent channel uses, for $\mathsf{M} \to \infty$, the P-SP bound is

$$\begin{aligned}\mathsf{C} &\leq \overline{\mathsf{C}}_{\text{P-SP}} \\ &\triangleq \min_{\substack{u,\\ u+l=2\mathsf{N}}} \sup_{\alpha \in [0,1]} \{\ell_U(\alpha) + \ell_L(\alpha)\} - \mathsf{N}\log(2\pi e\sigma_z^2),\end{aligned} \tag{24}$$

where $\ell_U(\alpha)$ is

$$\begin{aligned}\ell_U(\alpha) \triangleq \sup_{\theta \in [0,1]} \Bigg\{ &- u \sup_t \left\{ \theta t - \frac{1}{u} \log \sum_{j=0}^{u} \mathrm{V}_j\left(\Lambda_U \mathcal{X}_U\right) e^{jt} \right\} \\ &+ (1-\theta)\frac{u}{2} \log \frac{2\pi e\sigma_z^2}{1-\theta} \Bigg\},\end{aligned} \tag{25}$$

with Λ_U being the $u \times u$ submatrix of Λ with diagonal elements $\lambda_1, \ldots, \lambda_u$ and $\mathcal{X}_U = r\sqrt{1-\alpha^2}\mathcal{B}_u$. Moreover, $\ell_L(\alpha)$ is

$$\ell_L(\alpha) \triangleq \sum_{k=1}^{l} \frac{1}{2} \log\left(2\pi e\left(\lambda_{u+k}^2 \mathsf{P}_k(\alpha) + \sigma_z^2\right)\right), \tag{26}$$

where $\mathsf{P}_k(\alpha)$ is the power allocation given by the water-filling algorithm, for l parallel channels and a total power $\alpha^2 r^2$ allocated according to $\sigma_z^2/\lambda_{u+1}^2, \ldots, \sigma_z^2/\lambda_{2\mathsf{N}}^2$.

Proof: See Appendix C. □

Remark 2: When $\mathcal{X}$ is not a ball the asymptotic gap at high SNR between the P-SP upper bound and the EPI lower bound is larger than zero. On the other hand, if $\mathcal{X}$ is a ball we can again claim that the asymptotic gap is zero. Indeed, notice that whenever $\mathcal{X}$ is a ball and $u = 2\mathsf{N}$, the P-SP becomes equivalent to the SP upper bound, which we have shown having an asymptotically vanishing gap in Proposition 1.

VI. Case Studies

We now evaluate the performance of the SP upper bounds subject to specific constraints, induced by common transmitter configurations. Specifically, let us focus on two mentioned cases of practical interest, namely the *total amplitude* (TA) and the *per-antenna* (PA) constraints.

A. Total Amplitude Constraint

Let us evaluate the SP upper bound of Section V for the TA input constraint region $\mathcal{X} = \mathsf{A}\mathcal{B}_{2\mathsf{N}}$, with constraint amplitude $\mathsf{A} \in \mathbb{R}_+$. As shown in Theorem 1, to evaluate the bound $\overline{\mathsf{C}}_{\text{SP}}$ we need to be able to compute the intrinsic volumes $\mathrm{V}_j(\mathsf{H}\mathcal{X})$, for $j = 0, \ldots, 2\mathsf{N}$. As mentioned in Appendix C, when $\mathcal{X}$ is a ball, by considering the singular value decomposition of $\mathsf{H} = \mathsf{U}\Lambda\mathsf{V}^T$, it holds

$$\mathrm{V}_j(\mathsf{H}\mathcal{X}) = \mathrm{V}_j(\Lambda\mathcal{X}), \quad \forall j. \tag{27}$$

In [30], it is shown that given an ellipsoid

$$\mathcal{E} = \left\{ \mathbf{x} = [x_1, \ldots, x_{2\mathsf{N}}]^T \in \mathbb{R}^{2\mathsf{N}} : \mathbf{x}^T \Sigma^{-1} \mathbf{x} \leq 1 \right\}, \tag{28}$$

by defining j independent and identically distributed random vectors $\mathbf{Q}_1, \ldots, \mathbf{Q}_j \sim \mathcal{N}(\mathbf{0}_{2\mathsf{N}}, \Sigma)$ and the random matrix $\mathsf{Q} = [\mathbf{Q}_1, \ldots, \mathbf{Q}_j]$, it is possible to compute the jth intrinsic volume of $\mathcal{E}$ as

$$\mathrm{V}_j(\mathcal{E}) = \frac{(2\pi)^{j/2}}{j!} \mathsf{E}\left[\sqrt{\det\left(\mathsf{Q}^T \cdot \mathsf{Q}\right)}\right]. \tag{29}$$

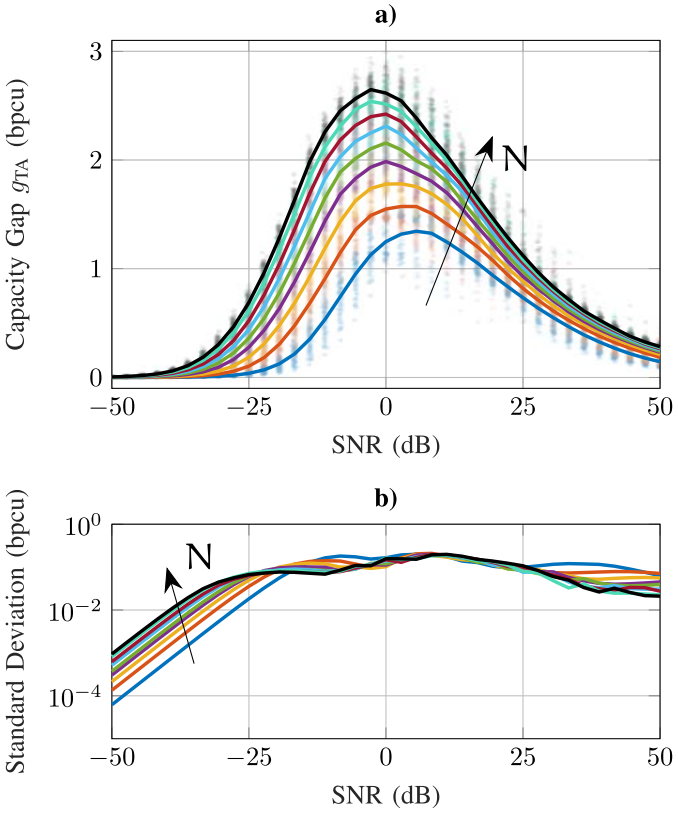

Fig. 3. **a)** Numerical evaluation of the capacity gap g_{TA}, defined in (31), in bit per channel use (bpcu) versus SNR, for $\mathsf{N} = 2, \ldots, 10$. For each N, the filled circles are the gaps resulting from each random channel realization, while the solid lines show the averaged behavior. **b)** Standard deviation of g_{TA} in bpcu versus SNR, for $\mathsf{N} = 2, \ldots, 10$.

Let us set $\Sigma = \Lambda^2$. Then, the intrinsic volumes for the TA configuration are given by

$$\mathrm{V}_j\left(\mathsf{H}\mathcal{X}\right) \overset{(3)}{=} \mathrm{V}_j\left(\mathcal{E}\right) \mathsf{A}^j, \qquad j = 0, \ldots, 2\mathsf{N}. \tag{30}$$

Given the intrinsic volumes in (30), we can use Theorem 1 to evaluate the SP upper bound for the TA constraint. Finally, to improve the performance of the SP bound at low SNR, we can apply the P-SP upper bound defined in Lemma 2.

Capacity Gap and Performance: To evaluate the gap we consider the piecewise-EPI (P-EPI) lower bound proposed in [20] and we denote it with $\underline{\mathsf{C}}_{\mathrm{TA}}$. Let us define the gap as

$$g_{\mathrm{TA}} \triangleq \overline{\mathsf{C}}_{\mathrm{TA}} - \underline{\mathsf{C}}_{\mathrm{TA}}, \tag{31}$$

where $\overline{\mathsf{C}}_{\mathrm{TA}}$ is given by the P-SP upper bound in Lemma 2, applied to the TA constraint. We evaluate g_{TA} numerically by Monte Carlo simulation for $\mathsf{N} = 2, \ldots, 10$, over random channel realizations. The entries of $\widetilde{\mathsf{H}}$ in (9) are drawn independently as $\widetilde{H}_{i,j} \sim \mathcal{CN}(0, 2),\ \forall i, j$.

The results are presented in Figs. 3–5. In Fig. 3a, we show a scatter plot of the gap realizations and with the solid lines the average gap, both versus SNR and for each $\mathsf{N} = 2, \ldots, 10$. In Fig. 3b, it is shown the standard deviation of g_{TA} for each N. As expected, when the SNR goes to zero the gap becomes small, because (24) is optimized by $u = 0$ and $\overline{\mathsf{C}}_{\mathrm{TA}}$ turns into the Gaussian maximum entropy bound, which is tight at low SNR. Moreover, the gap tends to decrease at high SNR. The gap eventually goes to zero, as stated in Remark 2, thanks to Proposition 1. Even in the worst case, g_{TA} is approximately 3 bit per channel use (bpcu). In both Fig. 4 and Fig. 5 we show that as N increases the performance of the upper bound improves. In Fig. 4, it is reported the average gap per complex dimension N in solid lines, while in Fig. 5 we show the expected ratio between the bounding gap and the upper bound. In Fig. 4, we also compare the gap of the proposed bound with the one resulting from the duality upper bounds of [19] defined in (13) and (14). Given $\overline{\mathsf{C}}_{\mathrm{D,TA}} \triangleq \min\left(\overline{\mathsf{C}}_{\mathrm{D},1}, \overline{\mathsf{C}}_{\mathrm{D},2}\right)$, the capacity gap for the duality upper bounds is given by

$$g_{\mathrm{D,TA}} \triangleq \overline{\mathsf{C}}_{\mathrm{D,TA}} - \underline{\mathsf{C}}_{\mathrm{TA}}. \tag{32}$$

The dashed lines in Fig. 4 are the average gaps for complex dimension $\mathsf{E}\left[g_{\mathrm{D,TA}}\right]/\mathsf{N}$, which are larger than $\mathsf{E}\left[g_{\mathrm{TA}}\right]/\mathsf{N}$ for any SNR level. Finally, in Fig. 6 we show the capacity bounds for a random channel realization given $\mathsf{N} = 10$.

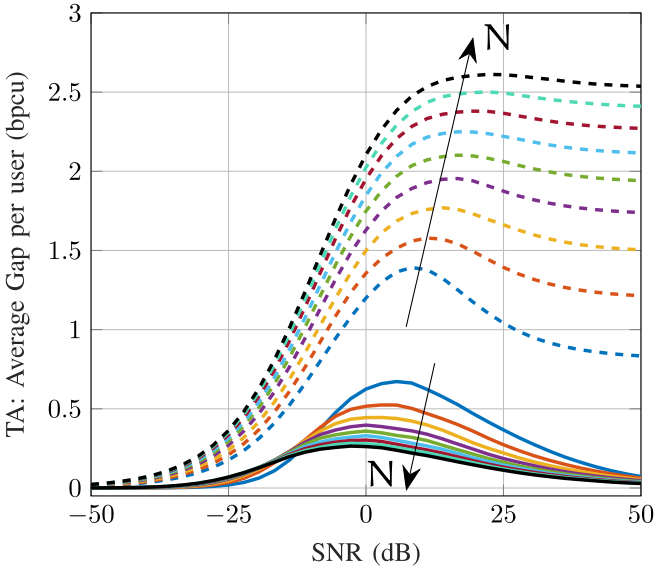

Fig. 4. Numerical evaluation of the average capacity gap per complex dimension in bit per channel use (bpcu) versus SNR, for $\mathsf{N} = 2, \ldots, 10$. The solid lines are $\mathsf{E}\left[g_{\mathrm{TA}}\right]/\mathsf{N}$, with g_{TA} defined in (31). The dashed lines are $\mathsf{E}\left[g_{\mathrm{D,TA}}\right]/\mathsf{N}$, with $g_{\mathrm{D,TA}}$ defined in (32).

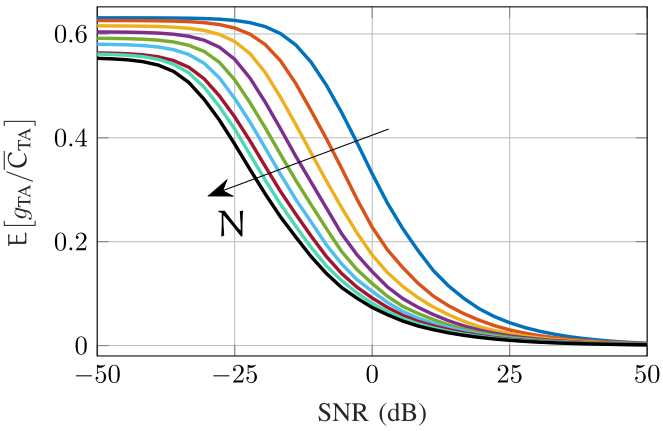

Fig. 5. Numerical evaluation of the average ratio between the capacity gap g_{TA}, defined in (31), and the upper bound $\overline{\mathsf{C}}_{\mathrm{TA}}$, derived from (24). The average ratio is plotted versus the SNR and for $\mathsf{N} = 2, \ldots, 10$.

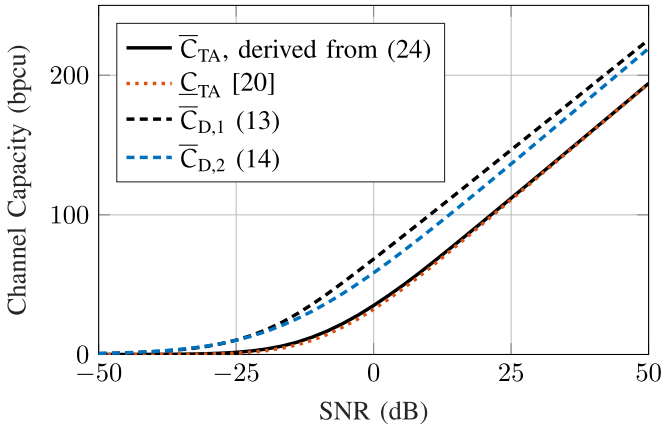

Fig. 6. Capacity bounds in bit per channel use (bpcu) versus SNR, for $\mathsf{N} = 10$ and for a random realization of the complex matrix H.

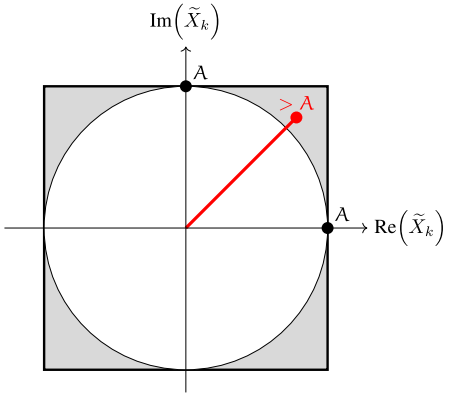

Fig. 7. Resulting constraint region for the complex input (circle) and for the real and imaginary part of the signal, independently (square).

The figure shows both how close our P-SP bound is to the lower bound and also the substantial improvement compared to $\overline{\mathsf{C}}_{\mathrm{D},1}$ and $\overline{\mathsf{C}}_{\mathrm{D},2}$.

B. Per-Antenna Constraint

Let us now consider the PA constraint. The complex input is such that $\widetilde{\mathbf{X}} \in \widetilde{\mathcal{X}} = \mathrm{Box}_{\mathsf{N}}\left(2\boldsymbol{\mathsf{A}}\right)$, with $\boldsymbol{\mathsf{A}} = (\mathsf{A}_1, \ldots, \mathsf{A}_{\mathsf{N}}) \in \mathbb{R}_+^{\mathsf{N}}$ being the vector of amplitude constraints. Since we can always consider an equivalent system by absorbing unequal A_k's in the channel matrix, we can assume $\mathsf{A}_k = \mathsf{A}, \forall k$ without loss of generality. Notice that constraining each entry of the vectorized input vector does not induce the same constraint as $\widetilde{\mathcal{X}}$. Applying the constraint on the entries of $\mathbf{X}$, and therefore after the vectorization of (9) like in [19], increases the capacity. Indeed, Fig. 7 shows that the constraint on the real and imaginary parts of $\widetilde{X}_k$ is weaker if compared to $\left|\widetilde{X}_k\right| \leq \mathsf{A}$, therefore it would induce a larger capacity. We think that in the case of wireless communication systems, where transmitted and received signals have a complex base-band representation, applying the constraint on $\widetilde{\mathbf{X}}$, instead of $\mathbf{X}$, correctly interprets the technological limitations imposed by power amplifiers. Notice that, on the other hand, free-space optical communication systems typically deal with intensity signals [4], [5], [6], [7], [8], then in that case the constraint would be applied directly on a real-valued input. In this case study, we focus on wireless systems, therefore the equivalent N real 2-dimensional constraints induced by $\left|\widetilde{X}_k\right| \leq \mathsf{A}$ are

$$\left[\mathrm{Re}\left(\widetilde{X}_k\right), \mathrm{Im}\left(\widetilde{X}_k\right)\right] \in \mathcal{X}_k = \mathsf{A}\mathcal{B}_2, \ \forall k = 1, \ldots, \mathsf{N}. \quad (33)$$

We remark that, given the PA constraint, the set $\mathcal{X}$ is then defined as the Cartesian product of N circles, $\mathcal{X} \triangleq \mathcal{X}_1 \times \cdots \times \mathcal{X}_{\mathsf{N}}$. Although it is fairly easy to evaluate the intrinsic volumes $\mathrm{V}_j\left(\mathcal{X}\right)$, the channel matrix H can distort $\mathcal{X}$ in such a way that $\mathsf{H}\mathcal{X}$ is not anymore a Cartesian product. Because of this distortion, even when the intrinsic volumes of $\mathcal{X}$ are known, it is not trivial to evaluate those of $\mathsf{H}\mathcal{X}$. Therefore, the only viable solution is to apply the G-SP bound by deriving upper bounds on $\mathrm{V}_j\left(\mathsf{H}\mathcal{X}\right)$.

Let us substitute each $\mathcal{X}_k$ with a larger region $\mathcal{R}_k = \mathrm{Box}_2\left(2\mathsf{A}\right) \supset \mathcal{X}_k, \ \forall k = 1, \ldots, \mathsf{N}$. Then we have

$$\mathcal{R} = \mathcal{R}_1 \times \cdots \times \mathcal{R}_{\mathsf{N}} = \mathrm{Box}_{2\mathsf{N}}\left(2\mathsf{A}\right) \supset \mathcal{X}. \quad (34)$$

We now show that it is possible to evaluate an upper bound on the intrinsic volumes $\mathrm{V}_j\left(\mathsf{H}\mathcal{R}\right)$ and therefore to derive a G-SP bound for the PA constraint. Let $\mathcal{P}$ be a $(2\mathsf{N})$-dimensional polytope and let $\mathbb{F}_j(\mathcal{P})$ denote the set of all j-dimensional faces of $\mathcal{P}$. From [27], the intrinsic volumes of a polytope are defined as

$$\mathrm{V}_j\left(\mathcal{P}\right) = \sum_{\mathcal{F} \in \mathbb{F}_j(\mathcal{P})} \gamma(\mathcal{F}, \mathcal{P}) \mathrm{Vol}_j\left(\mathcal{F}\right), \quad (35)$$

where $\gamma(\mathcal{F}, \mathcal{P})$ is the normalized external angle[2] of $\mathcal{P}$ at its face $\mathcal{F}$. Note that, since $\gamma(\mathcal{F}, \mathcal{P}) \leq 1$, we can upper-bound and simplify (35) with

$$\mathrm{V}_j\left(\mathcal{P}\right) \leq \sum_{\mathcal{F} \in \mathbb{F}_j(\mathcal{P})} \mathrm{Vol}_j\left(\mathcal{F}\right). \quad (36)$$

Notice that $\mathcal{R}$ is a parallelepiped, therefore by using (36) and results from exterior algebra, it is possible to evaluate an upper bound on $\mathrm{V}_j\left(\mathsf{H}\mathcal{R}\right)$. The authors of [32] show how a j-dimensional parallelepiped, with $j \leq 2\mathsf{N}$, can be identified by a set of j vectors $\mathbf{r}_1, \ldots, \mathbf{r}_j \in \mathbb{R}^{2\mathsf{N}}$ and by a base point $\mathbf{p} \in \mathbb{R}^{2\mathsf{N}}$. Let $\mathbf{p}$ be one of the vertices of the parallelepiped and let $\mathbf{r}_1, \ldots, \mathbf{r}_j$ have the same magnitude and direction of the j edges originating from $\mathbf{p}$. Then, the parallelepiped is composed of all points in $\mathbb{R}^{2\mathsf{N}}$ resulting from

$$\mathbf{p} + t_1\mathbf{r}_1 + \cdots + t_j\mathbf{r}_j, \quad 0 \leq t_1, \ldots, t_j \leq 1. \quad (37)$$

For instance, in Fig. 8 it is shown the three-dimensional parallelepiped spanned by linear combinations of the vectors $\mathbf{r}_1$, $\mathbf{r}_2$, and $\mathbf{r}_3$ given the base point $\mathbf{p}$. Since volume is invariant with respect to translations, we can drop the base point $\mathbf{p}$ and represent the geometric region $\mathcal{R}$ via the corresponding matrix R. Let us define it as

$$\mathsf{R} \triangleq \begin{bmatrix} \mathbf{r}_1 & \mathbf{r}_2 & \ldots & \mathbf{r}_{2\mathsf{N}} \end{bmatrix} = 2\mathsf{A} \cdot \mathsf{I}_{2\mathsf{N}}. \quad (38)$$

To evaluate the jth intrinsic volumes $\mathrm{V}_j\left(\mathcal{R}\right)$, with $j \leq 2\mathsf{N}$, we need to compute the j-dimensional volumes of all the faces spanned by all the possible combinations of j column vectors in R, accounting for all possible repetitions. Let us denote by $\mathcal{R}_{j,i}$ the j-dimensional face spanned by the ith

[2]For a more rigorous definition of external angle, see [31].

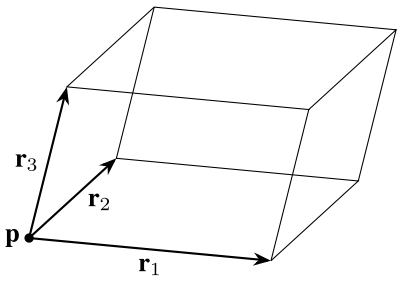

Fig. 8. Parallelepiped spanned by $\mathbf{r}_1$, $\mathbf{r}_2$, and $\mathbf{r}_3$ in $\mathbf{p}$.

combination of j column vectors in R, out of $\binom{2\mathsf{N}}{j}$. For instance, let us consider $\mathcal{R}_{j,1}$ to be the face spanned by the $\mathbf{r}_k$'s with $k = 1, \ldots, j$. Then, the corresponding $2\mathsf{N} \times j$ matrix is $\mathsf{R}_{j,1} = \begin{bmatrix}\mathbf{r}_1 & \mathbf{r}_2 & \ldots & \mathbf{r}_j\end{bmatrix}$. As shown in [32], the j-dimensional volume of the face $\mathcal{R}_{j,1}$ is given by

$$\mathrm{Vol}_j\left(\mathcal{R}_{j,1}\right) = \sqrt{\left|\det\left(\mathsf{R}_{j,1}^T \cdot \mathsf{R}_{j,1}\right)\right|}. \tag{39}$$

The same reasoning can be extended to any ith combination and it can be applied analogously after the distortion introduced by the channel matrix H. Let us define the region $\mathcal{S} = \mathsf{H}\mathcal{R} \supset \mathsf{H}\mathcal{X}$ and the corresponding $2\mathsf{N} \times 2\mathsf{N}$ matrix $\mathsf{S} = \begin{bmatrix}\mathsf{s}_1 & \mathsf{s}_2 & \ldots & \mathsf{s}_{2\mathsf{N}}\end{bmatrix} = \mathsf{H} \cdot \mathsf{R}$. Let $\mathcal{S}_A$ be the region characterized by the same intrinsic volumes of $\mathcal{S}$, but with external angles always equal to 1. Then by (36), the jth intrinsic volume of $\mathcal{S}$ can be upper-bounded by

$$\mathrm{V}_j\left(\mathcal{S}\right) \leq \mathrm{V}_j\left(\mathcal{S}_A\right) = 2^{2\mathsf{N}-j} \sum_{i=1}^{\binom{2\mathsf{N}}{j}} \sqrt{\left|\det\left(\mathsf{S}_{j,i}^T \cdot \mathsf{S}_{j,i}\right)\right|}, \tag{40}$$

where the term $2^{2\mathsf{N}-j}$ accounts for how many times each j-dimensional face is repeated in any parallelepiped. Since $\mathrm{V}_j\left(\mathsf{H}\mathcal{X}\right) \leq \mathrm{V}_j\left(\mathcal{S}\right) \leq \mathrm{V}_j\left(\mathcal{S}_A\right)$, (40) provides us with all the elements needed to apply the G-SP of Section V-A.

Another suitable upper bound on the intrinsic volumes of $\mathsf{H}\mathcal{X}$ can be derived by considering a region $\mathcal{S}_B \triangleq \mathsf{H}r_{\max}\left(\mathcal{X}\right)\mathcal{B}_{2\mathsf{N}} = \mathsf{H}\mathsf{A}\sqrt{\mathsf{N}}\mathcal{B}_{2\mathsf{N}} \supset \mathsf{H}\mathcal{X}$. Since $\mathcal{S}_B$ is an ellipsoid, its intrinsic volumes are easily derived as

$$\mathrm{V}_j\left(\mathcal{S}_B\right) = \mathrm{V}_j\left(\mathcal{E}\right)\left(\mathsf{A}\sqrt{\mathsf{N}}\right)^j, \tag{41}$$

where $\mathrm{V}_j\left(\mathcal{E}\right)$ is defined in (29), with $\Sigma = \Lambda^2$ and $\mathsf{H} = \mathsf{U}\Lambda\mathsf{V}^T$. Since both $\mathcal{S}_B$ and $\mathcal{S}_A$ can provide valid upper bounds, we choose the best option between (40) and (41) for each j, *i.e.*,

$$\overline{\mathrm{V}}_j = \begin{cases} 1, & j = 0, \\ \min\left(\mathrm{V}_j\left(\mathcal{S}_A\right), \mathrm{V}_j\left(\mathcal{S}_B\right)\right), & j = 1, \ldots, 2\mathsf{N}-1, \\ \det\left(\mathsf{H}\right)\mathrm{Vol}_{2\mathsf{N}}\left(\mathcal{X}\right), & j = 2\mathsf{N}. \end{cases} \tag{42}$$

Then, we can use the upper bound on the intrinsic volumes of $\mathsf{H}\mathcal{X}$ in (42) to evaluate the G-SP upper bound in Lemma 1 for the PA constraint, namely $\overline{\mathsf{C}}_{\mathrm{PA},1}$. Notice that $\overline{\mathrm{V}}_{2\mathsf{N}}$ is the true $(2\mathsf{N})$th intrinsic volume and it is given by $\overline{\mathrm{V}}_{2\mathsf{N}} = \det\left(\mathsf{H}\right)\mathrm{Vol}_{2\mathsf{N}}\left(\mathcal{X}\right) = \det\left(\mathsf{H}\right)\pi^{\mathsf{N}}\mathsf{A}^{2\mathsf{N}}$. Finally, by considering $r_{\max}\left(\mathcal{X}\right)\mathcal{B}_{2\mathsf{N}} = \mathsf{A}\sqrt{\mathsf{N}}\mathcal{B}_{2\mathsf{N}} \supset \mathcal{X}$, we can also evaluate the P-SP bound in Lemma 2 for the PA constraint, which we will denote by $\overline{\mathsf{C}}_{\mathrm{PA},2}$.

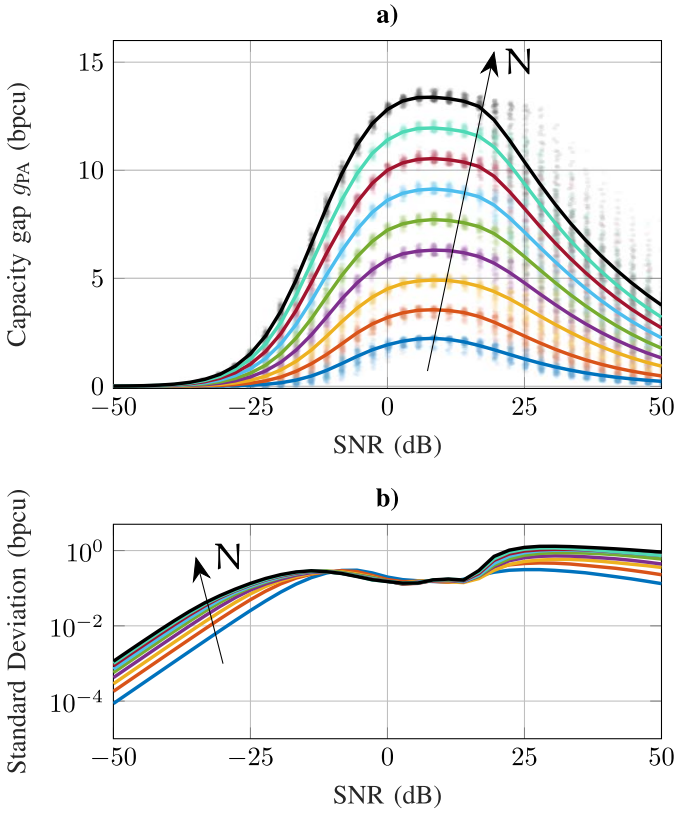

Fig. 9. **a)** Numerical evaluation of the capacity gap g_{PA}, defined in (43), in bit per channel use (bpcu) versus SNR, for $\mathsf{N} = 2, \ldots, 10$. For each N, the filled circles are the gaps resulting from each random channel realization, while the solid lines show the averaged behavior. **b)** Standard deviation of g_{PA} in bpcu versus SNR, for $\mathsf{N} = 2, \ldots, 10$.

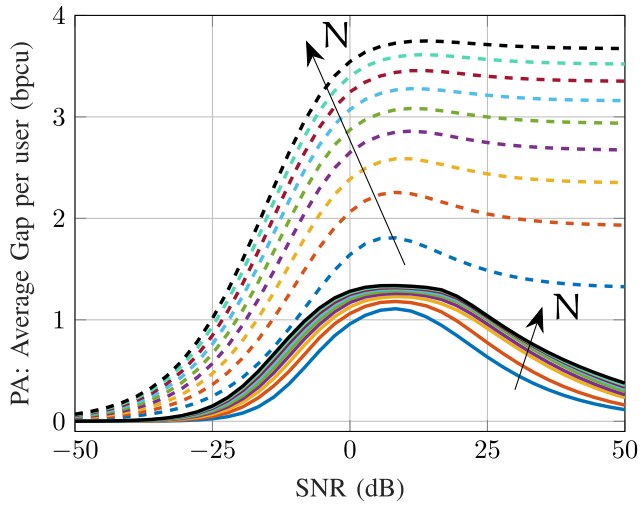

Fig. 10. Numerical evaluation of the average capacity gap per complex dimension in bit per channel use (bpcu) versus SNR, for $\mathsf{N} = 2, \ldots, 10$. The solid lines are $\mathsf{E}\left[g_{\mathrm{PA}}\right]/\mathsf{N}$, with g_{PA} defined in (43). The dashed lines are $\mathsf{E}\left[g_{\mathrm{D,PA}}\right]/\mathsf{N}$, with $g_{\mathrm{D,PA}}$ defined in (45).

Capacity Gap and Performance: Let us define the capacity gap for the PA constraint as

$$g_{\mathrm{PA}} \triangleq \overline{\mathsf{C}}_{\mathrm{PA}} - \underline{\mathsf{C}}_{\mathrm{PA}}, \tag{43}$$

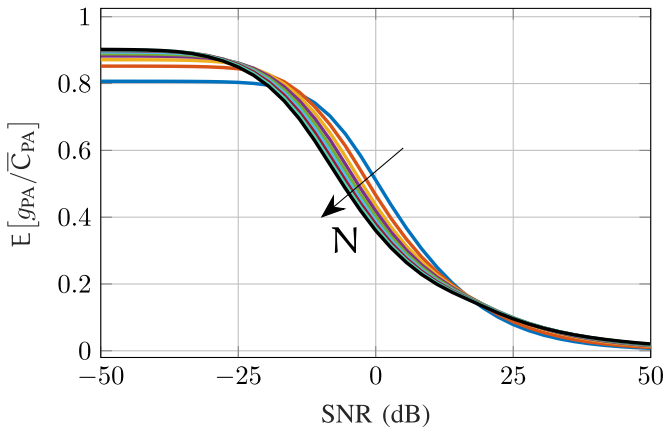

Fig. 11. Numerical evaluation of the average ratio between the capacity gap g_{PA}, defined in (43), and the upper bound $\overline{\mathsf{C}}_{\mathrm{PA}}$, defined in (44). The average ratio is plotted versus the SNR and for $\mathsf{N} = 2, \ldots, 10$.

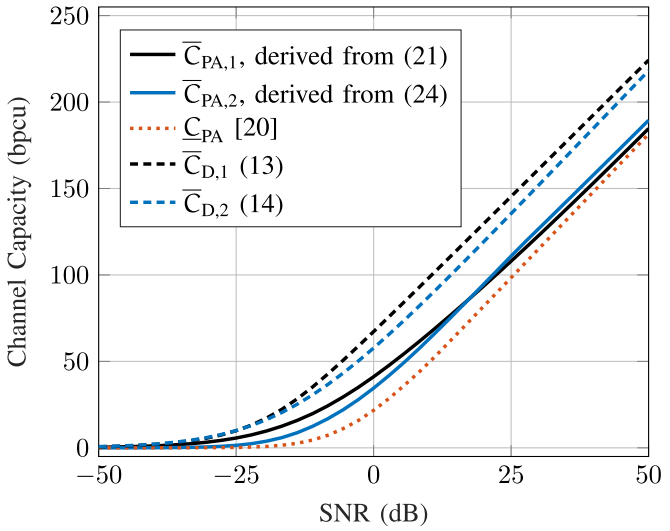

Fig. 12. Capacity bounds in bit per channel use (bpcu) versus SNR, for $\mathsf{N} = 10$ and for a random realization of the complex matrix $\widetilde{\mathsf{H}}$.

where $\underline{\mathsf{C}}_{\mathrm{PA}}$ is the P-EPI lower bound for the PA constraint from [20] and $\overline{\mathsf{C}}_{\mathrm{PA}}$ is given by

$$\overline{\mathsf{C}}_{\mathrm{PA}} = \min\left(\overline{\mathsf{C}}_{\mathrm{PA},1}, \overline{\mathsf{C}}_{\mathrm{PA},2}\right). \tag{44}$$

Fig. 9a shows a scatter plot of the gap realizations and, with solid lines, the averaged behavior. Both are shown versus the SNR, for $\mathsf{N} = 2, \ldots, 10$, and evaluated over random channel matrix realizations. The entries of $\widetilde{\mathsf{H}}$ in (9) are drawn independently as $\widetilde{H}_{i,j} \sim \mathcal{CN}(0, 2)$, $\forall i, j$. In Fig. 9b, we show the standard deviation of g_{PA} for each N. Fig. 9a shows that, like for the TA constraint, the gap is small for SNR going to zero thanks to the P-SP approach and tends to decrease at high SNR. As the SNR approaches infinity, the gap eventually goes to zero thanks to the G-SP approach, see Proposition 2. Notice that the capacity gap for the PA constraint, shown in Fig. 9a, is larger than the one resulting from the TA constraint, shown in Fig. 3a. This does not come as a surprise, it is simply due to the infeasibility in the direct evaluation of the intrinsic volumes of $\mathsf{H}\mathcal{X}$ and the consequent necessity to upper-bound them via the G-SP and P-SP approaches. Nevertheless, in Fig. 11 we show that the average ratio between the gap g_{PA} and the upper bound $\overline{\mathsf{C}}_{\mathrm{PA}}$ is within ≈ 0.1 after an SNR of 25 dB. Furthermore, Fig. 10 and Fig. 12 clearly show the benefits that the presented upper bounds provide if compared to the duality upper bounds of [19]. Like for the TA constraint, the upper bounds $\overline{\mathsf{C}}_{\mathrm{D},1}$ and $\overline{\mathsf{C}}_{\mathrm{D},2}$ are derived from [19, Theorem 10] and defined in (13) and (14) respectively. We remark that (14) requires the evaluation of the smallest box containing the region $\mathsf{H}\mathcal{X}$, which is not always a trivial task. Therefore, as we did for $\overline{\mathsf{C}}_{\mathrm{PA},2}$, in the derivation of $\overline{\mathsf{C}}_{\mathrm{D},2}$ for the PA constraint we made the simplifying assumption of considering an input constraint region $r_{\max}(\mathcal{X})\,\mathcal{B}_{2\mathsf{N}} = \mathsf{A}\sqrt{\mathsf{N}}\mathcal{B}_{2\mathsf{N}} \supset \mathcal{X}$. Then, we define $\overline{\mathsf{C}}_{\mathrm{D,PA}} \triangleq \min\left(\overline{\mathsf{C}}_{\mathrm{D},1}, \overline{\mathsf{C}}_{\mathrm{D},2}\right)$ and the capacity gap

$$g_{\mathrm{D,PA}} \triangleq \overline{\mathsf{C}}_{\mathrm{D,PA}} - \underline{\mathsf{C}}_{\mathrm{PA}}. \tag{45}$$

In Fig. 10, we show how the average gap per complex dimension given by g_{PA} is always smaller than that derived from $g_{\mathrm{D,PA}}$. Finally, in Fig. 12 we show the capacity bounds for a random channel realization, given $\mathsf{N} = 10$. Like for the TA constraint, it can be seen how the bound $\overline{\mathsf{C}}_{\mathrm{PA}}$ improves significantly upon the upper bounds $\overline{\mathsf{C}}_{\mathrm{D},1}$ and $\overline{\mathsf{C}}_{\mathrm{D},2}$ of [19].

VII. Conclusion

We derived an upper bound on the channel capacity of multiple-input multiple-output (MIMO) systems affected by fading and subject to peak amplitude constraints at the transmitter. We also introduced two variants of the proposed upper bound. One is used to always ensure a feasible evaluation of the bound and the other improves the performance at low signal-to-noise ratio (SNR). Moreover, we specialized the upper bounds for two particular constraints induced by practical transmitter configurations. The first configuration considers a transmitter employing a single power amplifier and determines a constraint on the norm of the input vector. The other configuration utilizes multiple amplifiers, one per transmitting antenna and it induces a constraint on the peak amplitude of each entry of the input vector. We proved that, for both configurations, the average capacity gap between the upper bounds and the best available lower bound, tends to vanish at high SNR. Moreover, we numerically showed that the capacity gap is finite virtually at any SNR level and for any of the considered MIMO dimensions. We also showed that the presented bounds represent a substantial improvement compared to the previously available upper bounds. Furthermore, we proved that the presented upper bounds are asymptotically tight at high SNR, not only for the considered constraints, but also for any peak amplitude convex constraint, for any channel matrix realization, and any dimension of the MIMO system.

Appendix A
Proof of Theorem 1

By [23, Theorem 3], we have that

$$\mathsf{C} \leq \limsup_{\mathsf{M}\to\infty} \frac{1}{\mathsf{M}} \log \frac{\mathrm{Vol}_n\left([\mathsf{H}\mathcal{X}]^{\times\mathsf{M}} \oplus \delta\mathcal{B}_n\right)}{\mathrm{Vol}_n\left(\delta\mathcal{B}_n\right)} \tag{46}$$

$$= \limsup_{\mathsf{M}\to\infty} \frac{1}{\mathsf{M}} \log \mathrm{Vol}_n\left([\mathsf{H}\mathcal{X}]^{\times\mathsf{M}} \oplus \delta\mathcal{B}_n\right) - \lim_{\mathsf{M}\to\infty} \frac{1}{\mathsf{M}} \log \mathrm{Vol}_n\left(\delta\mathcal{B}_n\right) \tag{47}$$

$$= \limsup_{\mathsf{M}\to\infty} \frac{1}{\mathsf{M}} \log \mathrm{Vol}_n \left([\mathsf{H}\mathcal{X}]^{\times \mathsf{M}} \oplus \delta \mathcal{B}_n \right) - \mathsf{N} \log \left(2\pi e \sigma_z^2 \right), \quad (48)$$

where $n = 2\mathsf{N}\mathsf{M}$ and $\delta = \sqrt{n\sigma_z^2}$. Let us focus on the evaluation of the limit superior. To deal with the convolution in (48) involving the output signal space $\mathcal{K} = [\mathsf{H}\mathcal{X}]^{\times \mathsf{M}}$, we define the limiting normalized generating function of the intrinsic volumes of $\mathcal{K}$, $f(t)$, as

$$f(t) \triangleq \lim_{\mathsf{M}\to\infty} \frac{1}{2\mathsf{N}\mathsf{M}} G_{\mathcal{K}}(t) \quad (49)$$

$$= \lim_{\mathsf{M}\to\infty} \frac{1}{2\mathsf{N}\mathsf{M}} G_{[\mathsf{H}\mathcal{X}]^{\times \mathsf{M}}}(t) \quad (50)$$

$$\overset{(7)}{=} \lim_{\mathsf{M}\to\infty} \frac{\mathsf{M}}{2\mathsf{N}\mathsf{M}} G_{\mathsf{H}\mathcal{X}}(t) \quad (51)$$

$$= \frac{1}{2\mathsf{N}} \log \left(\sum_{j=0}^{2\mathsf{N}} \mathrm{V}_j \left(\mathsf{H}\mathcal{X} \right) e^{jt} \right), \quad (52)$$

where $\overset{(7)}{=}$ indicates that (51) holds thanks to (7). Note that since $\mathsf{H}\mathcal{X}$ is a finite set, the intrinsic volumes $\mathrm{V}_j(\mathsf{H}\mathcal{X})$ exist and are finite, therefore the limit in (49) always exists. Thanks to (5), we have that

$$\mathrm{Vol}_n \left([\mathsf{H}\mathcal{X}]^{\times \mathsf{M}} \oplus \delta \mathcal{B}_n \right) = \sum_{j=0}^{n} \mathrm{V}_j \left(\mathcal{K} \right) \mathrm{Vol}_{n-j} \left(\delta \mathcal{B}_{n-j} \right). \quad (53)$$

As shown in [23], we can rewrite Steiner's formula as follows. Let us introduce the functions $a_n(\theta)$ and $b_n(\theta)$ with support $\theta \in [0,1]$. The function $a_n(\theta)$ is defined as the linear interpolation of the values

$$a_n(j/n) = \frac{1}{n} \log \mathrm{V}_j \left(\mathcal{K} \right), \quad j = 0, \ldots, n. \quad (54)$$

Given $a_n(\theta)$, let us define the sequence of measures

$$\widetilde{\mathrm{V}}_n \left(\theta \right) \triangleq e^{n a_n(\theta)}, \quad \theta \in [0,1]. \quad (55)$$

The function $b_n(\theta)$ is defined as

$$b_n(\theta) = \frac{1}{n} \log \frac{\pi^{n(1-\theta)/2}}{\Gamma\left(n(1-\theta)/2 + 1 \right)} \delta^{n(1-\theta)}, \quad \theta \in [0,1]. \quad (56)$$

Loosely speaking, the function $a_n(\theta)$ accounts for the intrinsic volumes in (53), while $b_n(\theta)$ accounts for $\mathrm{Vol}_{n-j}(\delta \mathcal{B}_{n-j})$. Let us define a function $v_n : [0,1] \to \mathbb{R}$ as

$$v_n(\theta) \triangleq a_n(\theta) + b_n(\theta). \quad (57)$$

Then, we can rewrite (53) as

$$\mathrm{Vol}_n \left([\mathsf{H}\mathcal{X}]^{\times \mathsf{M}} \oplus \delta \mathcal{B}_n \right) = \sum_{j=0}^{n} e^{n v_n(j/n)}. \quad (58)$$

We now want to prove that v_n converges for $\mathsf{M} \to \infty$. Notice that if both a_n and b_n converge, then also v_n converges. Let us start with a_n. Let f^* be the convex conjugate of f in (49), as defined in (8). By [23, Lemma 14], we have that given a closed set $I \subseteq \mathbb{R}$ it holds the large deviations upper bound

$$\limsup_{n\to\infty} \frac{1}{n} \log \widetilde{\mathrm{V}}_n \left(I \right) = \limsup_{n\to\infty} a_n(I) \leq - \inf_{t \in I} f^*(t), \quad (59)$$

and given an open set $F \subseteq \mathbb{R}$ it holds the large deviations lower bound

$$\limsup_{n\to\infty} \frac{1}{n} \log \widetilde{\mathrm{V}}_n \left(F \right) = \limsup_{n\to\infty} a_n(F) \geq - \inf_{t \in F} f^*(t). \quad (60)$$

Notice that these bounds require that the limit $f(t)$ exists for any $t \in \mathbb{R}$ and that $f(0) < \infty$. By (52), it is clear that, in our case, these requirements are always satisfied. Thanks to the concavity of $a_n(\cdot)$ for each n [23, Lemma 13], (59), and (60) we have

$$\lim_{n\to\infty} a_n(\theta) = -f^*(\theta). \quad (61)$$

For further detail, see the proof of [23, Lemma 15]. As for b_n, we also have

$$\lim_{n\to\infty} b_n(\theta) = \frac{1-\theta}{2} \log \frac{2\pi e \sigma_z^2}{1-\theta}. \quad (62)$$

Finally, since v_n is the sum of a_n and b_n we have

$$v(\theta) \triangleq \lim_{n\to\infty} v_n(\theta) = -f^*(\theta) + \frac{1-\theta}{2} \log \frac{2\pi e \sigma_z^2}{1-\theta}. \quad (63)$$

Let us now define

$$\hat{\theta}_n = \arg \max_{\theta \in [0,1]} v_n(\theta). \quad (64)$$

Notice that by (58) and thanks to the monotonicity of the logarithm, we can define the following upper and lower bounds

$$\frac{1}{\mathsf{M}} \log \left(e^{n v_n\left(\hat{\theta}_n\right)} \right) \leq \frac{1}{\mathsf{M}} \log \mathrm{Vol}_n \left([\mathsf{H}\mathcal{X}]^{\times \mathsf{M}} \oplus \delta \mathcal{B}_n \right) \quad (65a)$$

$$\leq \frac{1}{\mathsf{M}} \log \left((n+1) e^{n v_n\left(\hat{\theta}_n\right)} \right). \quad (65b)$$

By [23, Lemma 17] we have that

$$\lim_{n\to\infty} v_n \left(\hat{\theta}_n \right) = \sup_{\theta \in [0,1]} v(\theta). \quad (66)$$

Therefore, by taking the limit for $\mathsf{M} \to \infty$ of (65) and by noticing that

$$\lim_{\mathsf{M}\to\infty} \frac{1}{\mathsf{M}} \log \left(e^{n v_n\left(\hat{\theta}_n\right)} \right) = \lim_{\frac{n}{2\mathsf{N}} \to \infty} 2\mathsf{N} v_n \left(\hat{\theta}_n \right) \quad (67)$$

$$= 2\mathsf{N} \lim_{n\to\infty} v_n \left(\hat{\theta}_n \right), \quad (68)$$

we have that

$$2\mathsf{N} \sup_{\theta \in [0,1]} v(\theta) \leq \lim_{\mathsf{M}\to\infty} \frac{\log \mathrm{Vol}_n \left([\mathsf{H}\mathcal{X}]^{\times \mathsf{M}} \oplus \delta \mathcal{B}_n \right)}{\mathsf{M}} \quad (69a)$$

$$\leq 2\mathsf{N} \sup_{\theta \in [0,1]} v(\theta). \quad (69b)$$

We now have all the necessary elements to evaluate the limit superior in (48). For $\sigma_z^2 > 0$ it holds that

$$\ell(\sigma_z^2) \triangleq \limsup_{\mathsf{M}\to\infty} \frac{1}{\mathsf{M}} \log \mathrm{Vol}_n\left([\mathsf{H}\mathcal{X}]^{\times \mathsf{M}} \oplus \delta\mathcal{B}_n\right) \tag{70}$$

$$\overset{(69)}{=} \sup_{\theta} 2\mathsf{N}\cdot v(\theta) \tag{71}$$

$$\overset{(63)}{=} \sup_{\theta}\left\{-2\mathsf{N} f^*(\theta) + (1-\theta)\mathsf{N}\log\frac{2\pi e\sigma_z^2}{1-\theta}\right\} \tag{72}$$

$$\overset{(8)}{=} \sup_{\theta}\left\{-2\mathsf{N}\sup_t\{\theta t - f(t)\} + (1-\theta)\mathsf{N}\log\frac{2\pi e\sigma_z^2}{1-\theta}\right\} \tag{73}$$

$$\overset{(52)}{=} \sup_{\theta}\Bigg\{-\sup_t\left\{2\mathsf{N}\theta t - \log\left(\sum_{j=0}^{2\mathsf{N}} \mathrm{V}_j\left(\mathsf{H}\mathcal{X}\right) e^{jt}\right)\right\} + (1-\theta)\mathsf{N}\log\frac{2\pi e\sigma_z^2}{1-\theta}\Bigg\}, \tag{74}$$

where $\theta \in [0,1]$.

Appendix B
Proof of Proposition 1

Let us define

$$\theta^*(\sigma_z^2) = \arg\max_{\theta} v(\theta). \tag{75}$$

By [23, Lemma 18], we have that[3]

$$\limsup_{\sigma_z^2\to 0} \theta^*(\sigma_z^2) = 1. \tag{76}$$

Therefore it holds that

$$\lim_{\sigma_z^2\to 0} \ell(\sigma_z^2)$$

$$= -2\mathsf{N} f^*(1) \tag{77}$$

$$= -2\mathsf{N}\sup_t\left\{t - \frac{1}{2\mathsf{N}}\log\left(\sum_{j=0}^{2\mathsf{N}} \mathrm{V}_j\left(\mathsf{H}\mathcal{X}\right) e^{jt}\right)\right\} \tag{78}$$

$$= \inf_t\left\{\log\left(\sum_{j=0}^{2\mathsf{N}} \mathrm{V}_j\left(\mathsf{H}\mathcal{X}\right) e^{(j-2\mathsf{N})t}\right)\right\} \tag{79}$$

$$= \log\left(\inf_t\left\{\sum_{j=0}^{2\mathsf{N}} \mathrm{V}_j\left(\mathsf{H}\mathcal{X}\right) e^{(j-2\mathsf{N})t}\right\}\right) \tag{80}$$

$$= \log\left(\inf_t\left\{\sum_{j=0}^{2\mathsf{N}-1} \mathrm{V}_j\left(\mathsf{H}\mathcal{X}\right) e^{(j-2\mathsf{N})t}\right\} + \mathrm{V}_{2\mathsf{N}}\left(\mathsf{H}\mathcal{X}\right)\right) \tag{81}$$

$$= \log\left(\mathrm{Vol}_{2\mathsf{N}}\left(\mathsf{H}\mathcal{X}\right)\right), \tag{82}$$

where: i) (78) is a direct result of (8) and (52); ii) (80) holds thanks to the monotonicity of the logarithm; iii) (81) holds because, for $j = 2\mathsf{N}$, $\mathrm{V}_{2\mathsf{N}}\left(\mathsf{H}\mathcal{X}\right)$ can be taken out of the infimum operation; iv) (82) holds because the argument of the infimum in (81) is a sum of exponentials scaled by nonnegative coefficients, therefore the sum is minimized in $t\to\infty$ and the infimum is zero. The gap at high SNR results in

$$g_{\text{SP}} = \lim_{\sigma_z^2\to 0} \overline{\mathsf{C}}_{\text{SP}} - \underline{\mathsf{C}}_{\text{EPI}} \tag{83}$$

$$= \lim_{\sigma_z^2\to 0} \ell(\sigma_z^2) - \mathsf{N}\log\left(\left(\mathrm{Vol}_{2\mathsf{N}}\left(\mathsf{H}\mathcal{X}\right)\right)^{\frac{1}{\mathsf{N}}}\right) = 0. \tag{84}$$

[3]Note that we use a different notation compared to [23]. Specifically, the variable θ in [23] corresponds to $1-\theta$ in our work.

Appendix C
Proof of Lemma 2

Let us separate the MIMO channel into two independent subchannels. Then, we can apply the SP upper bound on one subchannel and the Gaussian maximum entropy bound on the other. Let us consider the singular value decomposition of $\mathsf{H} = \mathsf{U}\Lambda\mathsf{V}^T$ and let us define $\mathbf{Y}' = \mathsf{U}^{-1}\mathbf{Y}$, $\mathbf{X}' = \mathsf{V}^T\mathbf{X}$, and $\mathbf{Z}' = \mathsf{U}^{-1}\mathbf{Z}$ with $\mathbf{Z}' \sim \mathcal{N}(\mathbf{0}_{2\mathsf{N}}, \sigma_z^2\mathsf{I}_{2\mathsf{N}})$. An upper bound on the supremum of the entropy in (12) is given by

$$\sup_{F_{\mathbf{X}}:\,\mathbf{X}\in\mathcal{X}}\{\mathsf{h}(\mathbf{Y})\} = \sup_{F_{\mathbf{X}}:\,\mathbf{X}\in\mathcal{X}}\{\mathsf{h}(\mathbf{Y}')\} \tag{85}$$

$$= \sup_{F_{\mathbf{X}}:\,\mathbf{X}\in\mathcal{X}}\{\mathsf{h}(\mathbf{Y}_U, \mathbf{Y}_L)\} \tag{86}$$

$$\leq \sup_{F_{\mathbf{X}}:\,\mathbf{X}\in\mathcal{X}}\{\mathsf{h}(\mathbf{Y}_U) + \mathsf{h}(\mathbf{Y}_L)\}, \tag{87}$$

where $\mathbf{Y}' = \binom{\mathbf{Y}_U}{\mathbf{Y}_L}$, with $\mathbf{Y}_U = [Y_1', \ldots, Y_u']^T \in \mathbb{R}^u$, $\mathbf{Y}_L = \left[Y_{u+1}', \ldots, Y_{u+l}'\right]^T \in \mathbb{R}^l$, and $u+l = 2\mathsf{N}$. Furthermore, we have $\mathbf{X}' = \binom{\mathbf{X}_U}{\mathbf{X}_L}$, with $\mathbf{X}_U$ and $\mathbf{X}_L$ defined similarly to $\mathbf{Y}_U$ and $\mathbf{Y}_L$. We want to treat independently the contributions of $\mathsf{h}(\mathbf{Y}_U)$ and $\mathsf{h}(\mathbf{Y}_L)$, to upper-bound them with the two mentioned techniques. First, note that it holds

$$\mathrm{V}_j\left(\mathsf{H}\mathcal{X}\right) = \mathrm{V}_j\left(\Lambda\mathcal{X}\right), \quad \forall j. \tag{88}$$

Then, the subsystem to which $\mathbf{Y}_U$ belongs, perceives larger singular values, and therefore higher SNR. On the other hand, $\mathbf{Y}_L$ refers to the subsystem affected by a lower SNR due to smaller singular values. Then, we expect the SP upper bound to be more accurate on $\mathsf{h}(\mathbf{Y}_U)$, where the transmitted signal is stronger compared to the noise level, while we expect it to be less precise on $\mathsf{h}(\mathbf{Y}_L)$. Since in the subsystem of $\mathbf{Y}_L$ the Gaussian noise is dominant, a tighter upper bound on $\mathsf{h}(\mathbf{Y}_L)$ can be provided by the differential entropy of a Gaussian-distributed vector $\overline{\mathbf{Y}}_L \sim \mathcal{N}(\mathbf{0}_l, \Sigma_L)$, with $\Sigma_L = \Lambda_L\mathsf{E}\left[\mathbf{X}_L\mathbf{X}_L^T\right]\Lambda_L + \sigma_z^2\mathsf{I}_l$ and with Λ_L being the $l\times l$ submatrix of Λ with diagonal elements $\lambda_{u+1}, \ldots, \lambda_{2\mathsf{N}}$. Furthermore, to separate the capacity contributions of the two subsystems, we need to reformulate the input constraint in such a way that it can be separated as well. Let us assume $\mathcal{X}$ to be a ball and let us define its radius as $r = r_{\max}(\mathcal{X})$. Then, we have

$$\|\mathbf{X}\|^2 = \|\mathbf{X}_U\|^2 + \|\mathbf{X}_L\|^2 \leq r^2. \tag{89}$$

We reinterpret r^2 as $r^2(1-\alpha^2) + r^2\alpha^2$ with $\alpha \in [0,1]$. Therefore, the constraint $\|\mathbf{X}\| \leq r$ becomes equivalent to

$$\bigcup_{\alpha\in[0,1]}\left\{F_{\mathbf{X}}:\ \|\mathbf{X}_U\| \leq r\sqrt{1-\alpha^2},\ \|\mathbf{X}_L\| \leq r\alpha\right\}. \tag{90}$$

By plugging this equivalent constraint into (87), we obtain

$$\sup_{F_{\mathbf{X}}:\,\mathbf{X}\in\mathcal{X}} \{\mathsf{h}(\mathbf{Y}_U)+\mathsf{h}(\mathbf{Y}_L)\} \tag{91}$$

$$= \sup_{\alpha\in[0,1]} \left\{ \sup_{F_{\mathbf{X}}:\begin{cases}\|\mathbf{X}_U\|\le r\sqrt{1-\alpha^2}\\ \|\mathbf{X}_L\|\le r\alpha\end{cases}} \{\mathsf{h}(\mathbf{Y}_U)+\mathsf{h}(\mathbf{Y}_L)\} \right\} \tag{92}$$

$$= \sup_{\alpha\in[0,1]} \left\{ \sup_{F_{\mathbf{X}_U}:\,\|\mathbf{X}_U\|\le r\sqrt{1-\alpha^2}} \{\mathsf{h}(\mathbf{Y}_U)\} + \sup_{F_{\mathbf{X}_L}:\,\|\mathbf{X}_L\|\le r\alpha} \{\mathsf{h}(\mathbf{Y}_L)\} \right\}. \tag{93}$$

Then, we can apply the SP upper bound in (17) on the subsystem of $\mathbf{Y}_U$ to get

$$\sup_{F_{\mathbf{X}_U}:\,\|\mathbf{X}_U\|\le r\sqrt{1-\alpha^2}} \{\mathsf{h}(\mathbf{Y}_U)\} \le \ell_U(\alpha). \tag{94}$$

For the subsystem associated with $\mathbf{Y}_L$, the upper bound is given by

$$\sup_{F_{\mathbf{X}_L}:\,\|\mathbf{X}_L\|\le r\alpha} \mathsf{h}(\mathbf{Y}_L) \tag{95}$$

$$\le \sup_{F_{\mathbf{X}_L}:\,\|\mathbf{X}_L\|\le r\alpha} \mathsf{h}\left(\overline{\mathbf{Y}}_L\right) \tag{96}$$

$$\overset{(a)}{\le} \sup_{\mathsf{E}\left[\|\mathbf{X}_L\|^2\right]\le r^2\alpha^2} \mathsf{h}\left(\overline{\mathbf{Y}}_L\right) \tag{97}$$

$$\overset{(b)}{\le} \sup_{\mathsf{E}\left[\|\mathbf{X}_L\|^2\right]\le r^2\alpha^2} \sum_{k=1}^{l} \frac{1}{2}\log\left(2\pi e\left(\lambda_{u+k}^2\mathsf{E}\left[|X_{L,k}|^2\right]+\sigma_z^2\right)\right) \tag{98}$$

$$= \sum_{k=1}^{l} \frac{1}{2}\log\left(2\pi e\left(\lambda_{u+k}^2\mathsf{P}_k(\alpha)+\sigma_z^2\right)\right) \tag{99}$$

$$= \ell_L(\alpha), \tag{100}$$

where in (a) we replaced $\|\mathbf{X}_L\| \le r\alpha$ with the looser constraint $\mathsf{E}\left[\|\mathbf{X}_L\|^2\right] \le r^2\alpha^2$ and in (b) we used the fact that $\mathsf{h}\left(\overline{\mathbf{Y}}_L\right) \le \sum_k \mathsf{h}\left(\overline{Y}_{L,k}\right)$, with $\overline{Y}_{L,k}$ being the kth component of the vector $\overline{\mathbf{Y}}_L$. Moreover, similarly to $\overline{Y}_{L,k}$, we denote by $X_{L,k}$ the kth component of the vector $\mathbf{X}_L$ and by $\mathsf{P}_k(\alpha)$ the power allocation given by the water-filling algorithm, which maximizes (98) for the constraint $\mathsf{E}\left[\|\mathbf{X}_L\|^2\right] \le r^2\alpha^2$. Finally, notice that even when $\mathcal{X}$ is not a ball we can simply consider the enlarged constraint $r_{\max}(\mathcal{X})\mathcal{B}_{2\mathsf{N}} \supset \mathcal{X}$ instead of $\mathcal{X}$ and still provide a valid upper bound.

REFERENCES

[1] A. Favano, M. Ferrari, M. Magarini, and L. Barletta, "A sphere packing bound for AWGN MIMO fading channels under peak amplitude constraints," in *Proc. IEEE Inf. Theory Workshop (ITW)*, Apr. 2021, pp. 1–5.

[2] C. E. Shannon, "A mathematical theory of communication," *Bell Syst. Tech. J.*, vol. 27, no. 3, pp. 379–423, Jul. 1948.

[3] E. Telatar, "Capacity of multi-antenna Gaussian channels," *Eur. Trans. Telecommun.*, vol. 10, no. 6, pp. 585–595, Nov./Dec. 1999.

[4] A. Chaaban, J.-M. Morvan, and M.-S. Alouini, "Free-space optical communications: Capacity bounds, approximations, and a new sphere-packing perspective," *IEEE Trans. Commun.*, vol. 64, no. 3, pp. 1176–1191, Mar. 2016.

[5] L. Li, S. M. Moser, L. Wang, and M. Wigger, "On the capacity of MIMO optical wireless channels," *IEEE Trans. Inf. Theory*, vol. 66, no. 9, pp. 5660–5682, Sep. 2020.

[6] A. Lapidoth, S. M. Moser, and M. A. Wigger, "On the capacity of free-space optical intensity channels," *IEEE Trans. Inf. Theory*, vol. 55, no. 10, pp. 4449–4461, Oct. 2009.

[7] N. Sharma and S. S. Shamai, "Transition points in the capacity-achieving distribution for the peak-power limited AWGN and free-space optical intensity channels," *Problems Inf. Transmiss.*, vol. 46, no. 4, pp. 283–299, Dec. 2010.

[8] S. M. Moser, M. Mylonakis, L. Wang, and M. Wigger, "Asymptotic capacity results for MIMO wireless optical communication," in *Proc. IEEE Int. Symp. Inf. Theory (ISIT)*, Jun. 2017, pp. 536–540.

[9] J. G. Smith, "The information capacity of amplitude- and variance-constrained scalar Gaussian channels," *Inf. Control*, vol. 18, no. 3, pp. 203–219, Apr. 1971.

[10] S. S. Shamai and I. Bar-David, "The capacity of average and peak-power-limited quadrature Gaussian channels," *IEEE Trans. Inf. Theory*, vol. 41, no. 4, pp. 1060–1071, Jul. 1995.

[11] A. Tchamkerten, "On the discreteness of capacity-achieving distributions," *IEEE Trans. Inf. Theory*, vol. 50, no. 11, pp. 2773–2778, Nov. 2004.

[12] T. H. Chan, S. Hranilovic, and F. R. Kschischang, "Capacity-achieving probability measure for conditionally Gaussian channels with bounded inputs," *IEEE Trans. Inf. Theory*, vol. 51, no. 6, pp. 2073–2088, Jun. 2005.

[13] B. Mamandipoor, K. Moshksar, and A. K. Khandani, "Capacity-achieving distributions in Gaussian multiple access channel with peak power constraints," *IEEE Trans. Inf. Theory*, vol. 60, no. 10, pp. 6080–6092, Oct. 2014.

[14] A. L. McKellips, "Simple tight bounds on capacity for the peak-limited discrete-time channel," in *Proc. IEEE Int. Symp. Inf. Theory (ISIT)*, Jun./Jul. 2004, p. 348.

[15] B. Rassouli and B. Clerckx, "On the capacity of vector Gaussian channels with bounded inputs," *IEEE Trans. Inf. Theory*, vol. 62, no. 12, pp. 6884–6903, Dec. 2016.

[16] A. Thangaraj, G. Kramer, and G. Böcherer, "Capacity bounds for discrete-time, amplitude-constrained, additive white Gaussian noise channels," *IEEE Trans. Inf. Theory*, vol. 63, no. 7, pp. 4172–4182, Jul. 2017.

[17] A. Favano, M. Ferrari, M. Magarini, and L. Barletta, "The capacity of the amplitude-constrained vector Gaussian channel," in *Proc. IEEE Int. Symp. Inf. Theory (ISIT)*, Jul. 2021, pp. 426–431.

[18] A. ElMoslimany and T. M. Duman, "On the capacity of multiple-antenna systems and parallel Gaussian channels with amplitude-limited inputs," *IEEE Trans. Commun.*, vol. 64, no. 7, pp. 2888–2899, Jul. 2016.

[19] A. Dytso, M. Goldenbaum, H. V. Poor, and S. Shamai (Shitz), "Amplitude constrained mimo channels: Properties of optimal input distributions and bounds on the capacity," *Entropy*, vol. 21, no. 2, p. 200, Feb. 2019.

[20] A. Favano, M. Ferrari, M. Magarini, and L. Barletta, "Capacity bounds for amplitude-constrained AWGN MIMO channels with fading," in *Proc. IEEE Int. Symp. Inf. Theory (ISIT)*, Jun. 2020, pp. 2032–2037.

[21] K. N. R. S. V. Prasad, E. Hossain, and V. K. Bhargava, "Energy efficiency in massive MIMO-based 5G networks: Opportunities and challenges," *IEEE Wireless Commun.*, vol. 24, no. 3, pp. 86–94, Jun. 2017.

[22] S. Loyka, "The capacity of Gaussian MIMO channels under total and per-antenna power constraints," *IEEE Trans. Commun.*, vol. 65, no. 3, pp. 1035–1043, Mar. 2017.

[23] V. Jog and V. Anantharam, "A geometric analysis of the AWGN channel with a (σ,ρ)-power constraint," *IEEE Trans. Inf. Theory*, vol. 62, no. 8, pp. 4413–4438, Aug. 2016.

[24] M. Lotz, M. B. McCoy, I. Nourdin, G. Peccati, and J. A. Tropp, "Concentration of the intrinsic volumes of a convex body," in *Geometric Aspects of Functional Analysis: Israel Seminar (GAFA) 2017-2019*, vol. 2. Cham, Switzerland: Springer, Jul. 2020, pp. 139–167.

[25] J. B. Conway, *A Course in Functional Analysis*, vol. 96. New York, NY, USA: Springer, 2019.

[26] M. Henk and M. A. H. Cifre, "Intrinsic volumes and successive radii," *J. Math. Anal. Appl.*, vol. 343, no. 2, pp. 733–742, Jul. 2008.

[27] P. McMullen, "Non-linear angle-sum relations for polyhedral cones and polytopes," *Math. Proc. Cambridge Phil. Soc.*, vol. 78, no. 2, pp. 247–261, Sep. 1975.

[28] R. Schneider, *Convex Bodies: The Brunn–Minkowski Theory*. Cambridge, U.K.: Cambridge Univ. Press, 2014, no. 151.

[29] R. T. Rockafellar, *Convex Analysis*, vol. 36. Princeton, NJ: Princeton Univ. Press, Jan. 1997.
[30] D. Zaporozhets and Z. Kabluchko, "Random determinants, mixed volumes of ellipsoids, and zeros of Gaussian random fields," *J. Math. Sci.*, vol. 199, no. 2, pp. 168–173, May 2014.
[31] B. Grünbaum, "Grassmann angles of convex polytopes," *Acta Math.*, vol. 121, no. 1, pp. 293–302, 1968.
[32] M. Khosravi and M. D. Taylor, "The wedge product and analytic geometry," *Amer. Math. Monthly*, vol. 115, no. 7, pp. 623–644, Aug./Sep. 2008.

Antonino Favano (Member, IEEE) received the M.S. degree *(cum laude)* in telecommunication engineering from the Politecnico di Milano, Milan, Italy, in 2018. He is currently pursuing the dual Ph.D. degree in the information technology program with the Politecnico di Milano and the Istituto di Elettronica e di Ingegneria dell'Informazione e delle Telecomunicazioni (IEIIT), Consiglio Nazionale delle Ricerche (CNR). His research interests include the investigation of the channel capacity for wireless MIMO channels subject to amplitude constraints and in general, the broader theme of green communications.

Marco Ferrari (Member, IEEE) was born in Milano, Italy, in 1971. He received the Laurea degree (M.S. equivalent) *(cum laude)* in telecommunications engineering and the Ph.D. degree in electronics and communication engineering from the Politecnico di Milano, Italy, in 1996 and 2000, respectively. Since 2001, he has been a Researcher with the Institute Istituto di Elettronica e di Ingegneria dell'Informazione e delle Telecomunicazioni (IEIIT), Consiglio Nazionale delle Ricerche (CNR), Politecnico di Milano. In 2002, he was an EPRSC Research Fellow with the University of Plymouth, U.K. He has coauthored approximately 60 scientific publications on leading international journals and conference proceedings and few patents. His main research interests are in channel coding, information theory, and digital transmission. He is a member of the Communications and Information Theory Societies.

Maurizio Magarini (Member, IEEE) received the M.Sc. and Ph.D. degrees in electronic engineering from the Politecnico di Milano, Milan, Italy, in 1994 and 1999, respectively. In 1994, he was granted the TELECOM Italia Scholarship Award for his M.Sc. Thesis. He worked as a Research Associate with the Dipartimento di Elettronica, Informazione e Bioingegneria, Politecnico di Milano, from 1999 to 2001. From 2001 to 2018, he was an Assistant Professor with the Politecnico di Milano, where he has been an Associate Professor, since June 2018. From August 2008 to January 2009, he spent a sabbatical leave at the Bell Laboratories, Alcatel-Lucent, Holmdel, NJ, USA. His research interests are in the broad area of communication and information theory. Topics include synchronization, channel estimation, equalization, and coding applied to wireless and optical communication systems. His most recent research activities have focused on molecular communications, massive MIMO, study of waveforms for 5G cellular systems, vehicular communications, wireless sensor networks for mission critical applications, and wireless networks using unmanned aerial vehicles and high-altitude platforms. He has authored and coauthored more than 130 journals and conference papers. He was a co-recipient of two best-paper awards. He is an Associate Editor of IEEE ACCESS, *IET Electronics Letters*, and *Nano Communication Networks* (Elsevier). He has been involved in several European and National research projects.

Luca Barletta (Member, IEEE) received the M.S. degree *(cum laude)* in telecommunications engineering and the Ph.D. degree in information engineering from the Politecnico di Milano, Milano, Italy, in 2007 and 2011, respectively. In 2012, he was a Visiting Researcher at the Bell Laboratories, Alcatel-Lucent, Holmdel, NJ, USA, working on long-haul fiber-optic communications. From 2012 to 2015, he was a Post-Doctoral Researcher at the Institute for Advanced Study and Institute for Communications Engineering, Technische Universitaet Muenchen, Munich, Germany, working on capacity for continuous-time phase-noise channels. Since 2019, he has been with the Politecnico di Milano, where he is currently an Associate Professor, working in the broad field of information and communication theory. In 2020, he received the IEEE Communications Society Charles Kao Award for the paper "Machine-Learning Method for Quality of Transmission Prediction of Unestablished Lightpaths," appeared on the IEEE/OSA JOURNAL OF OPTICAL COMMUNICATIONS AND NETWORKING, Vol. 10, No. 2.

Open Access funding provided by 'Consiglio Nazionale delle Ricerche-CARI-CARE' within the CRUI CARE Agreement